Università
Ca'Foscari
Venezia
Facoltà
di Scienze
Matematiche
Fisiche e Naturali

Corso di Laurea Magistrale
in Scienze Chimiche per la Conservazione
e il Restauro

Prova finale di Laurea

Chemometric analysis of the photooxidative decolorization of the azo dye Acid Red 97

Relatore
Prof. R. Piazza
Prof. M. Pilar Callao Lasmarías

Correlatore
C. Fernández Barrat

Laureando
Daniela Iseppi
Matricola 811106

Anno Accademico
2011 / 2012

"sono qui perso su una piccola scrivania
a cercare di capire se quello che cerco
è in questo porto o altrove
ed a rimpiangere di non aver detto addio
ma solo un arrivederci"

(Andreas Terragni)

Alle mie radici

INDEX

ABBREVETIONS

A	Absorbance
AOPs	Advanced Oxidation Processes
A.R.97	Acid Red 97
EFA	Evolving Factor Analysis
EI	Electron Impact
ESI	Electrospray ionization
HOMO	Highest Occupied Molecular Orbital
LOF	Lack of fit
LUMO	Lowest Occupied Molecular Orbital
MCR-ALS	Multivariate Curve Resolution with Alternative Least Square
MS	Mass Spectrometry
PCA	Principal Component Analysis
r	Correlation coefficient
R^2	Percent of variance explained
SVD	Singular Value Decomposition
URV	Rovira i Virgilii University
UV	Ultraviolet

- 1 -

INTRODUCTION
AND OBJECTIVES

PURPOSE OF THE THESIS PROJECT

The work presented in this thesis was carried out at the Department of Analytical and Organic Chemistry of the Rovira i Virgilii University, URV (Tarragona, Spain), under the supervision of Professors M. Pilar Callao and M. Soledad Larrechi, members of the research group of Chemometric, Qualimetric and Nanosensors.

Since the October 2011, I have joined this research group by the active cooperation between Rovira i Virgili University and Ca' Foscari University (Venice, Italy), under the international Erasmus program. This cooperation was made possible by the efforts of the coordinators of URV and Ca' Foscari University, Prof. M. Elena Fernandez and Prof. A. Perosa, respectively.

The main object of the work undertaken was to learn chemometric techniques as multivariate curve resolution methods, with the aim to develop analytical methodology able to determine multiple compounds in a sample without specific analytical signal. This approach was applied in the analysis of the photodegradation process of an azo dye using UV-visible spectroscopy. It has allowed to go deep on a subject, azo dyes, already tackled during the academic studies, and to acquired or, for the first time, put in practise new knowledge in the matter of chemometric methods and analytical techniques.

This subject was approved as the project of my thesis degree by the Didactic College of the Master's Course *Chemical Science for Conservation and Restauration*, of Ca' Foscari University, with Prof. R. Piazza and Prof. M. Pilar Callao as relators.

As it will be discussed, the work developed is focused on a specifically environmental theme: the problem of the presence of azo dyes in wastewaters, their degradation and removal. However the methodology developed can find many applications also in the analysis of materials constituting cultural heritage objects. For example it could be used for the study of the ageing process of several materials or fot the study of kinetic degradation of those materials, used in contemporary art, of which future behavior is still unknown. In addition it could be applied in monitoring the conservation of cultural heritage objects.

OBIETTIVO DEL PROGETTO DI TESI

Il lavoro presentato in questa tesi è stato condotto presso il Dipartimento di Chimica Analitica ed Inorganica dell'Università Rovira i Virgilii, URV (Tarragona, Spagna), sotto la supervisione delle Professoresse M. Pilar Callao e M. Soledad Larecchi, membri del gruppo di ricerca di Chemiometria, Qualimetria e Nanosensori.

A partire da Ottobre 2011 ho potuto unirmi a questo gruppo di ricerca grazie al conseguimento di una borsa di studio referente al programma di scambio universitario inter-europeo Erasmus. Ciò ha permesso l'avvio di una cooperazione tra l'Università Rovira i Virgilli e l'Università Ca' Foscari (Venezia, Italia), siglata dai coordinatori Prof. M. Elena Fernandez e Prof. A. Perosa rispettivamente.

Lo scopo principale del lavoro intrapreso fu l'apprendimento di tecniche chemiometriche, tra cui metodi di risoluzione multivariata, al fine di sviluppare una metodologia analitica capace di determinare differenti composti presenti in un campione senza segnali analitici specifici.

In particolare tale approccio è stato applicato nell'analisi del processo di fotodegradazione di un azo colorante mediante spettroscopia UV-visibile. Ciò ha permesso di approfondire un argomento, quello degli azo coloranti, già incontrato durante gli studi accademici, e di acquisire o applicare per la prima volta nuove conoscenze riguardanti metodi chemiometrici e tecniche analitiche.

L'argomento sviluppato nel lavoro affrontato fu approvato come progetto di tesi magistrale dal Collegio Didattico del Corso di Laurea Magistrale *Scienze Chimiche per la Conservazione ed il Restauro* dell'Università Ca' Foscari, con Prof. R. Piazza e Prof. M. Pilar Callao in qualità di relatori.

Come verrà discusso a breve, il lavoro sviluppato si incentra su un tema di natura prettamente ambientale, vale a dire quello del problema della presenza degli azocoloranti nelle acque di refluo, del loro degrado e della loro rimozione. Tuttavia la metodica sviluppata può trovare molteplici applicazioni anche nell'ambito dell'analisi dei materiali costituenti gli oggetti di interessi storico-artistici. Ad esempio potrebbe essere impiegata per lo studio del processo di invecchiamento di diversi materiali o della cinetica di degradazione di quei materiali, utilizzati nell'arte contemporanea, dei quali è ancora ignoto il futuro comportamento. Inoltre tale metodologia potrebbe trovare applicazione nel monitoraggio dello stato di conservazione delle opere artistiche.

INTRODUCTION

Since last century dyes are widely used in industry and among them organic azo dyes seem to occupy an important place, due to the huge variability of their colors and thanks to their versatility in several fields (textile, leather, pharmaceutical, printing, plastics and food industries). It has been estimated that they account for 60-70% of the 10.000 commercial dyes currently in use [1].

Azo dyes are particularly used in textile industry where 20-25% of the initial dye contents are lost during dyeing process and released in effluents [2]. The presence of dyes in the wastewaters constitutes a serious environmental problem due to their reactivity, toxicity and recalcitrant, as many of them have low biodegradability under aerobic conditions. They can be hazardous for human health because of their mutagenic and carcinogenic properties.

For this reason, in the last years, several efforts have been put in with the aim to find new technologies for the removal of recalcitrant dyes which are effective and in the meantime economical and eco-friendly. Another important aspect is that normally wastewaters are a complex system composed not only of dyes, but also of a different inorganic constituents and auxiliary organic chemicals. Considering these aspects, different treatments based on either physical, chemical or biological principles have been studied. An important class of methodologies is the Advanced Oxidation Processes (AOPs) that are based on the generation of reactive species such as hydroxyl radicals and present the great advantage of no generating secondary pollution.

In this work an AOP homogeneous method, conducted without catalyst and with UV radiation in presence of oxygen peroxide, H_2O_2, is used for the degradation process of an acid azo dye, Acid Red 97. This last is one of the most used in the textile industry (Trumpler Española) that has provided the sample of dye used in the work.

The optimal conditions for rapid dye removal were already developed in a previous study [3]. The analysis has been carried out with chemometric tools and analytical instruments in order to identify the chemical intermediates produced during the process and, therefore, define a hypothetic reaction pathway.

Dye removal reaction was firstly monitored by UV-visible spectroscopy and then the collected spectra were treated by means of a Multivariate Curve Resolution method with Alternative Least Square (MCR-ALS). In this process, the number of

variability sources, related to the number of chemical species, was analysed using Singular Value Decomposition (SVD) and the Evolving Factor Analysis (EFA) of the UV-visible spectra recorded during the degradation. The information were complemented by Mass Spectrometry (MS) analysis of some represented samples, taken during the degradation process, in order to propose a reaction pathway.

Moreover it has been investigated the role of the concentration of H_2O_2 on the degradation trend, as it is one of the most important influential factors in the H_2O_2/UV photolysis.

INTRODUZIONE

A partire dal XX secolo i coloranti sintetici sono stati ampiamente impiegati in diversi settori dell'industria. Tra questi i coloranti azoici occupano un importante posto grazie alla grande varietà dei loro colori e per la loro versatilità che ne permette l'uso in diversi campi (nell'industria tessile, farmaceutica, plastica, nella lavorazione della pelle, ecc…). È stato stimato che gli azo coloranti costituiscono circa il 60-70% dei 10.000 coloranti commerciali attualmente in uso [1].

Gli azo coloranti sono particolarmente utilizzati nell'industria tessile dove si ipotizza che circa il 20-25% del loro contenuto iniziale non venga fissato sulla fibre e venga conseguentemente rilasciato nelle acque di refluo [2]. La presenza di azo coloranti nelle acque rappresenta un grave problema ambientale a causa della loro reattività, tossicità e per il fatto che molti di essi presentano una bassa biodegradabilità in condizioni aerobiche. È ormai certo che gli azo coloranti sono composti dannosi e pericolosi sia per l'ambiente che per gli esseri umani. Molti studi hanno dimostrato il loro potenziale cancerogeno e mutageno ai danni dell'uomo, nonché la loro azione di inibizione o rallentamento delle funzioni vitali di piante e animali.

Pertanto, negli ultimi anni la ricerca scientifica ha cercato di sviluppare metodologie atte alla rimozione dei coloranti presenti nelle acque di refluo, che siano efficaci ma al contempo anche economiche e che non determinino esse stesse un impatto ambientale. Occorre inoltre considerare che normalmente le acque di refluo costituiscono un sistema complesso dove si possono trovare, oltre ai coloranti, differenti composti inorganici e organici. Considerando questi aspetti sono state studiate diverse

metodologie basate su principi fisici, chimici e biologici. Tra queste particolare interesse è stato rivolto ai Processi di Ossidazione Avanzata (AOP) che prevedono la formazione di specie chimiche altamente reattive, quali radicali ossidrili, che promuovono la degradazione di substrati organici, arrivando ad ottenere una completa mineralizzazione senza la produzione di inquinanti secondari.

In particolare, in questo studio è stato utilizzato un processo di ossidazione omogenea, che prevede l'uso di radiazione UV in presenza di H_2O_2 come agente ossidante, per il processo di fotodegradazione dell'azo colorante Acid Red 97, uno dei più utilizzati dall'industria (Trumpler Española) che ha fornito il campione di colorante necessario per lo studio.

L'analisi del processo è stata condotta mediante l'uso di metodi chemiometrici e strumenti analitici con lo scopo di identificare gli intermedi chimici prodotti durante la degradazione e, pertanto, definire un ipotetico cammino di reazione.

Il processo di degradazione del colorante è stato prima monitorato mediante spettroscopia UV-visibile. I dati spettrali raccolti sono stati poi trattati per mezzo del metodo multivariante MCR-ALS (Multivariate Curve Resolution with Alternative Least Square). Tale approccio chemiometrico prevede che il numero delle fonti di variabilità, relative al numero delle specie chimiche prodotte nel processo, siano individuate applicando agli spettri UV-visibili raccolti l'algoritmo di Decomposizione a Valori Singoli (SVD) e l'Analisi dei Fattori in Evoluzione (EFA).

Le informazioni così ottenute sono state completate dall'analisi in spettrometria di massa (MS) di alcuni campioni raccolti durante il processo di degradazione.

Inoltre è stato investigato il ruolo assunto dalla concentrazione di H_2O_2 nell'andamento del processo di degradazione, essendo uno dei principali fattori che influenzano la fotolisi condotta con H_2O_2/UV.

- 2 -

THEORICAL
BACKGROUNDS

2.1 AZO-DYES AND ENVIROMENTAL PROBLEMS

This section contains an overview about azo dyes, their structure and properties, and the environmental problems connected with them. Moreover it is focused on acid dyes and in particular on Acid Red 97, which is the object studied in this investigation.

2.1.1 Azo dyes

2.1.1.1 Characteristics and synthesis

Azo dyes are characterized by the presence of the azo chromophoric group (-N=N-) which are usually associated with aromatic rings such as benzene or naphtalene derivatives. They contain also an electron-withdrawing and/or electrodonating groups as auxocromes generally in *meta* or *para* position respect to the azo group.

The synthesis of azo dyes is called *diazocopulation* and, normally, it involves two steps, (fig.2.1). In the first step, known as *diazotization*, an aromatic amine is converted to a diazo compound, using nitrous acid, HNO_2, produced by the reaction of an halogen acid with sodium nitrite, $NaNO_2$. The reaction activator is the nitrosonium ion, NO^+, an electrophile species, that forms a diazonium salt.

Subsequently the diazo compound formed reacts with coupling components (Ar'-H in the fig. 2.1), such as phenol, naphthol, aromatic amines, or compounds that have an active methylene group. This last process is known as *coupling* and leads to formation of the azo dyes [4, 5].
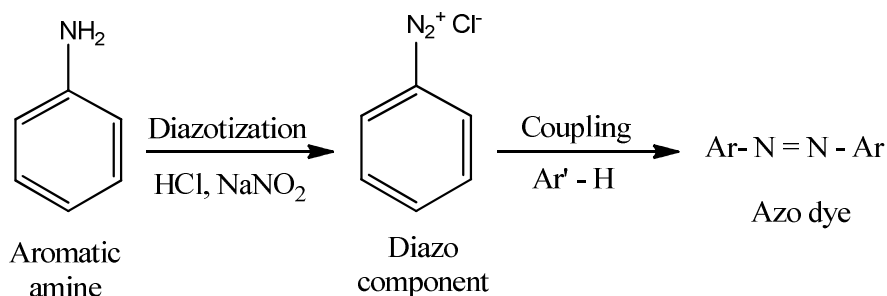
Fig. 2.1 Principal steps of the diazocopulation reaction.

2.1.1.2 The base of color

Unlike most organic compounds, dyes present a large variety of colors. This is due to different reasons depending on the molecular structure of dyes characterized by an elevate conjugation.

Dyes absorb light in the visible spectrum (400–700 nm), showing a color directly connected with the wavelength absorbed (Tab. 2.1). The energy of the visible radiation absorbed is sufficient to promote or excite a molecular electron to a higher-energy orbital.

Table 2.1 Relationship between visible wavelength absorbed and color observed.

WAVELENGTH ABSORBED (nm)	COLOR ABSORBED	COLOR OBSERVED
400-435	Violet	Yellow-green
435-480	Blue	Yellow
480-490	Green-blue	Orange
490-500	Blue-green	Red
500-560	Green	Purple
560-580	Yellow-green	Violet
580-595	Yellow	Blue
595-605	Orange	Green-blue
605-700	Red	Blue-green

Fig 2.2. shows the electronic excitations that may occur in organic molecules. Among these transitions, only the two lowest energy ones (the yellow arrows) are achieved by energies available in the 200 to 800 nm spectrum, i.e. visible and near ultraviolet regions. As a rule, energetically favored electron promotion will be from the Highest Occupied Molecular Orbital (HOMO) to the Lowest Unoccupied Molecular Orbital (LUMO) [6].
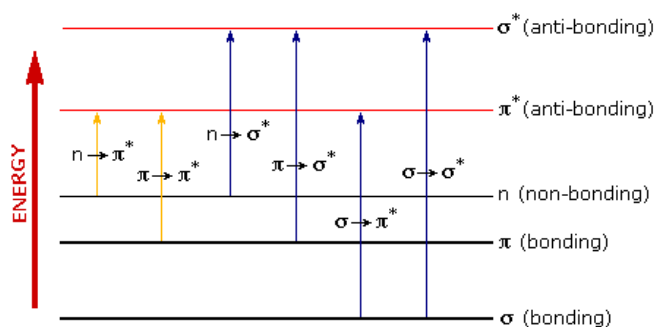
Fig. 2.2 Energetic levels of molecular orbitals

In particular this absorption, in the UV-visible range, is caused by the presence into the molecule of certain groups, called *chromophores*, that are generally pi-electron functions and hetero atoms having non-bonding valence-shell electron pairs. Important chromophores are: -N=N-, -C=O, -C=S, $-NO_2$, -CN, -C=N-, etc. When the molecule is exposed to light, having an energy that matches a possible molecular electronic transition, light is absorbed and color is visible.

However the presence of chromophore is not necessarily sufficient for color: it must be conjugated with an extensive system with alternating single and double bonds as exist in aromatic compounds.

In addition to chromophores, most dyes also contain groups known as *auxochromes*. A feature of these auxochromes is the presence of at least one lone pair of electrons which can be viewed as extending the conjugated system by resonance. Some examples are carboxylic acid, sulfonic acid, amino, and hydroxyl groups. While these are not responsible for color, their presence can shift the color of a colorant and they are most often used to influence dye solubility.

For what explained so far, it is clear that the color of dyes is directly connected with system contains extensively conjugative pi-electrons. In fact, an increase of the

conjugation into the same molecule, due to chromophores and auxochromes, leads to an increment of the resonance of electron cloud, bringing the HOMO and LUMO orbitals closer together. In this way, the energy required to effect the electron promotion is therefore less, and the wavelength that provides this energy is correspondingly increased.

2.1.1.3 Classification

All dyes and pigments are classified in the *Color Index International* [7-9], a reference database jointly maintained by the Society of Dyers and Colorists and the American Association of Textile Chemists and Colorists. The classification of pigments and dyes is based on their chemical composition, allowing to research a specific colorant on the basis of its physic-chemical properties. The individual colorants are identified in two ways: throughout the *Color Index Generic Name*, called C.I. Name, and with the use of *Color Index Number*, known as C.I. N°, formed by five numbers, that give additional information to the C.I. Name. For example the C.I. Name of Cobalt Blue is PB28 (Pigment Blue 28), while its C.I. Number is 77346.

In the Color Index azo dyes constitute the largest group of synthetic dyes and can be subdivided into monoazo, disazo, trisazo and polyazo derivatives with a specific assigned range of color index number [5, 7].

Another classification system is based in the bounding mechanism between dyes and fibers. Practically textile dyes are classified into: acid, basic, disperse, direct and reactive dyes. Table 2.2. (pag.15) presents an example for each azo-class, and their principal characteristics.

In particular acid dyes were so called for the presence in their molecules of one or more sulphonic acid groups generally salified with a Na. Attachment to the fibre is attributed at least partly to salt formation between anionic groups in the dyes and cationic groups in the fibre. They are used for polyamide and protein substrates such as nylon, wool, silk and leather, normally forming ionic bonds within the polymer matrix, bearing a positive charge, as shown in reaction 2.1 [10]:

$$\text{Dye-SO}_3^-\text{Na}^+ + \text{pol-NH}_3^+\text{Cl}^- \rightarrow \text{Dye-SO}_3^- + \text{H}_3\text{N-pol} \qquad (2.1)$$
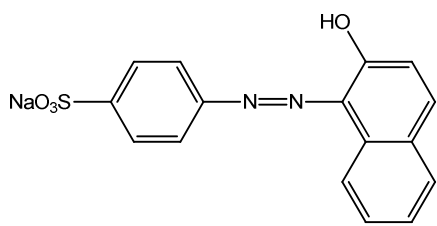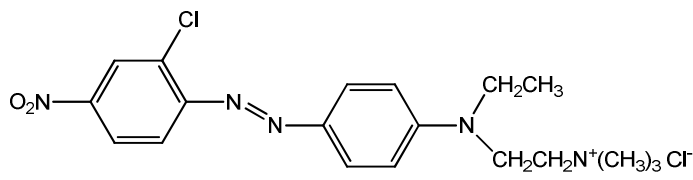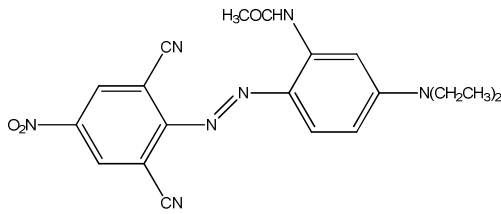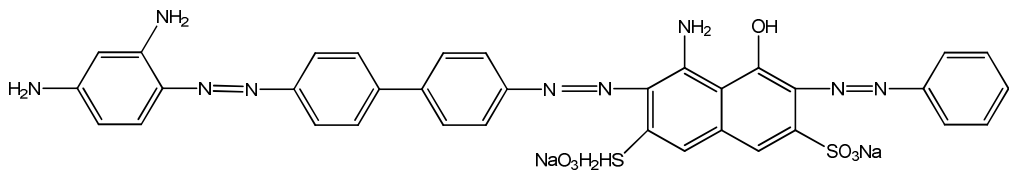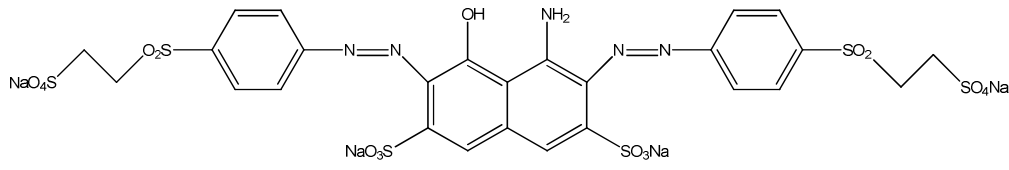
Basic dyes have amino groups, or alkyl amino groups, as their auxochromes, and consequently have an overall positive charge [11]. For this reason they are used with polymers such as poly(acrylonitrile) carring a negative (anionic) charge in their backbone. These dyes have no affinity for polyester, cellulosic, or polyamide polymers, since such substrates cannot form an ionic bond with them. However, cationic dyes can be used to dye protein fibres and, in fact, the first synthetic dye Mauveine, developed by William Henry Perkin in the 1856, was a basic dye that was used for dyeing silk [10].

Disperse dyes was developed for hydrophobic substrates such as polyester and acetate. In this case the dye is dissolved in the polymer matrix to form a solid–solid solution. Such colorants are very sparingly soluble in water and derive their name from the fact that they are dispersed rather than fully dissolved in water to carry out the dyeing process.

Direct dyes are so named because they were the first colorants that had affinity for cotton in the absence of a mordant. The molecular base of these dyes is benzidine and, for this, they are also called benzidine-based direct dyes. Some direct dyes have extensive uses other than on cellulose fibres, many being of outstanding importance for use on paper, leather, wool, silk and nylon.

Finally reactive dyes derive their name from the fact that they undergo a chemical reaction with cellulose to form a covalent bond. They are applied in weakly acid conditions, under which reaction with the fibers does not occur. Dyeing is then readily obtained on treatment with alkali, a reaction with the fiber takes place and the resulting dyeing is very fast to wet treatments.

Tab. 2.2 Examples and characteristics of the principal azo-dye classes.

DYE CLASS	CHARACTERISTICS	APPLICATION	DYE-FIBRE ATTACHMENT MECHANISM
Acid	Anionic, water soluble	Nylon, wool	Ionic bond, Van des Waals

ACID ORANGE 7 (C.I. 15510)

Basic	Cationic, water soluble	Acrylic, nylon, silk cotton, wool	Ionic bond

BASIC RED 18 (C.I. 11085)

Disperse	Colloidal dispersion, very low water solubility	Polyester, nylon, acetate, cellulose, acrylic	Solid solution formation

DISPERSIVE BLUE 165 (C.I. 63285)

Direct	Anionic, water soluble	Cotton	H-bond

DIRECT BLACK 38 (C.I. 30235)

Reactive	Anionic, water soluble	Cotton, silk, nylon, wool	Covalent bond

REACTIVE BLACK 5 (C.I. 20505)

18

2.1.2 Acid Red 97

The Acid Red 97 (dye A.R.97) is widely used in textile and tuning industries. Fig.2.4 shows the chemical structure of this dye: it is a polyprotic molecule, characterized by a benzidine, with sulphonate functional groups, linked through azo bonds to two naphthalene rings. The azo bonds (red circles) constitute the chromophore in the molecule, while sulphonic acid groups (green rectangle) make the dye highly soluble. For this dye it is possible to suppose the existence of a azo-hydrazone tautomer pair (Fig.2.5), since it contains –OH and an azo group in neighbouring position [12].

C.I. Name
Acid Red 97
C.I. Number
22890
Molecular Formula
$C_{32}H_{20}N_4Na_2O_8S_2$
λ max
497 nm
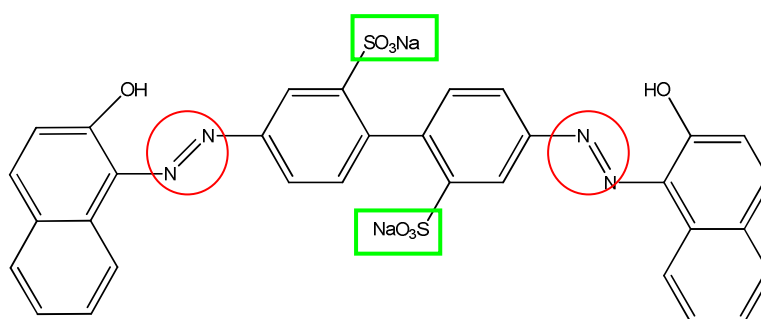
Fig. 2.4 Molecular structure and principal characteristics of dye Acid Red 97.
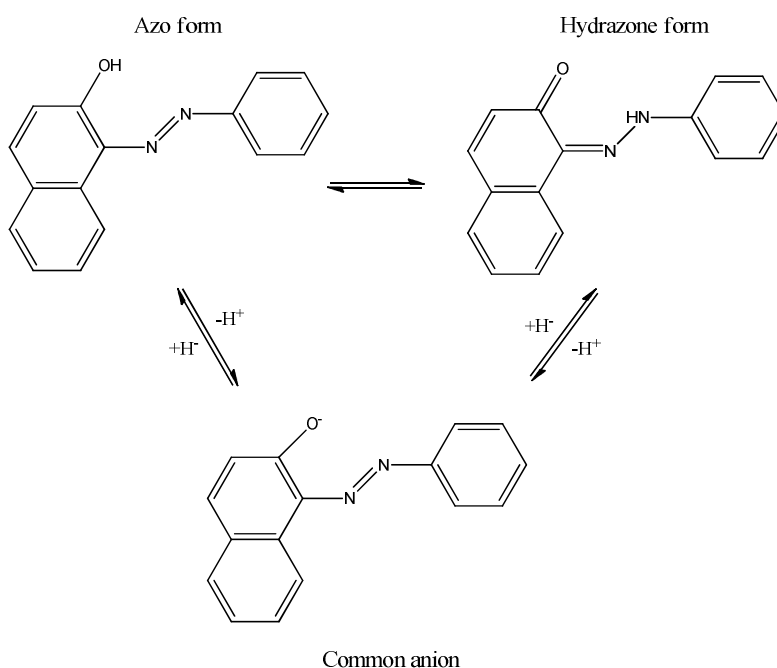
Fig. 2.5 Hypothetic azo-hydrazone tautomerism exhibited by AR97.

2.1.3 Environmental problems of azo dyes

It has been estimated that more than 10% of the total dyestuff used in dyeing processes does not bind to the fibres and is released in the environment. In particular the overwhelming majority of synthetic dyes currently used in the industry are azo derivatives, constituting 60-70 % of all dyestuff produced [1].

Azo dyes are widely used in textile, printing and dye houses due to their easy of production, fastness and variety of colors compared to natural dyes. Because of their chemical structure, that is also responsible for intense color, they are characterized by high water solubility and resistance to degradation under natural conditions. Due to these characteristics and to their large-scale production and extensive application, azo dyes can cause considerable environmental pollution, making them hazardous compounds not only for the acute effects on flora and fauna but also for human health [13].

In particular it has been studied that the reductive splitting of azo dyes (Fig. 2.6) can lead to the release of carcinogenic aromatic amines, that are generally not degraded and accumulate under anaerobic conditions. Furthermore benzidine based dyes have long been recognized has an hazard carcinogen.
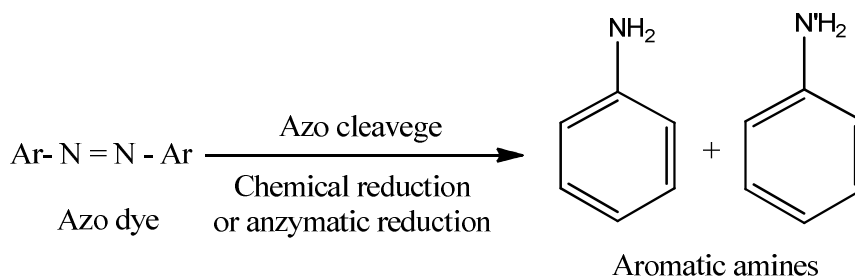
Fig. 2.6 Reductive splitting of azo dye.

Reductive cleavage conditions can be found in a reductive chemical medium (chemical reduction) and in living organism as a result of the action of intestinal bacteria or azoreducatase (enzymatic reduction) [14, 15].

In light of these characteristics it is understandable that the presence of dyes in water bodies represents a relevant problem that leads to several negative consequences.

Firstly they have a visual anaesthetic impact even at low concentration. This abnormal coloration impedes light penetration in the water, upsetting photosynthesis and, in general, normal biological processes within a stream [16]. In particular it has been proved that effluents of some of dyes commonly used reduce the rate of seed germination and growth of crop plants, as a consequence of the decrease of the level of dissolved oxygen. Moreover decrease of chlorophyll contents can be attributed to higher concentrations of dissolved solids or increase in chlorophyllase, an enzyme responsible for chlorophyll degradation, or decrease of endogenous cytokines acid (ABA), that normally is involved in chlorophyll synthesis. Many studies have also demonstrated the toxicity of several dyes for fish and shellfish [15].

The assumption of dyes by plants and organisms in the water leads to a dangerous bioaccumulation that may eventually affect human by transport through the food chain. This causes various physiological disorders like hypertension, renal damage, cramps, etc. Especially in the recent years the role of azo dyes in causing cancer has been investigated. It is suppose that the ultimate carcinogen arises from the metabolic conversion of aromatic amines and azo compounds to electrophilic species that interact with electron-rich sites in DNA causing DNA adducts, mutations and subsequent adverse effects on the cell. It is also clear that ring substituents that enhance the hydrophobic character increase carcinogenic potential [10].

2.2 AZO-DYES REMOVAL TECHNIQUES

So far it has been focused on the several problems caused by colorants in water. For this reason legislation about toxic substances in industrial wastewaters is becoming increasingly strict. Consequently there was a remarkable development in the research of new, economic and low environmental impact methodologies for removal of textile wastewaters.

A lot of methodologies have been developed in order to resolve this problem (Fig.2.7). In general dyes-containing wastewaters can be treated in two ways: non-destructive, that includes physic techniques, and destructive, that refers to biodegradation and to Advanced Oxidation Processes (AOPs), i.e. chemical methods [17]. Moreover a combination of processes are usually applied in order to meet regulatory discharge limits, exploiting the advantages of different techniques [18].

This section is organized in three parts. In the first part the physicochemical and biological techniques are briefly described. In the second one the AOPs are introduced, as it deals with the most used and investigated methodologies during the last years. More space is dedicated to an accurate discussion about H_2O_2 photolysis, since it is the technic applied in this study.

TREATMENT METHODS
FOR AZO DYES

PHYSICAL METHODS	CHEMICAL METHODS	BIOLOGICAL METHODS

PHYSICAL METHODS
- Adsorption
- Coagulation/floculation
- Electrocoagulation
- Filtration
- Reverse Osmosis

CHEMICAL METHODS

AOP processes

Non irradiation:
- Ozonation
- Electrochemical oxidation
- Direct oxidation
- Fenton's reaction

Irradiation:
- Photolysis
- Photocatalysys

BIOLOGICAL METHODS
- Bacteria
- Fungus
- Enzymas

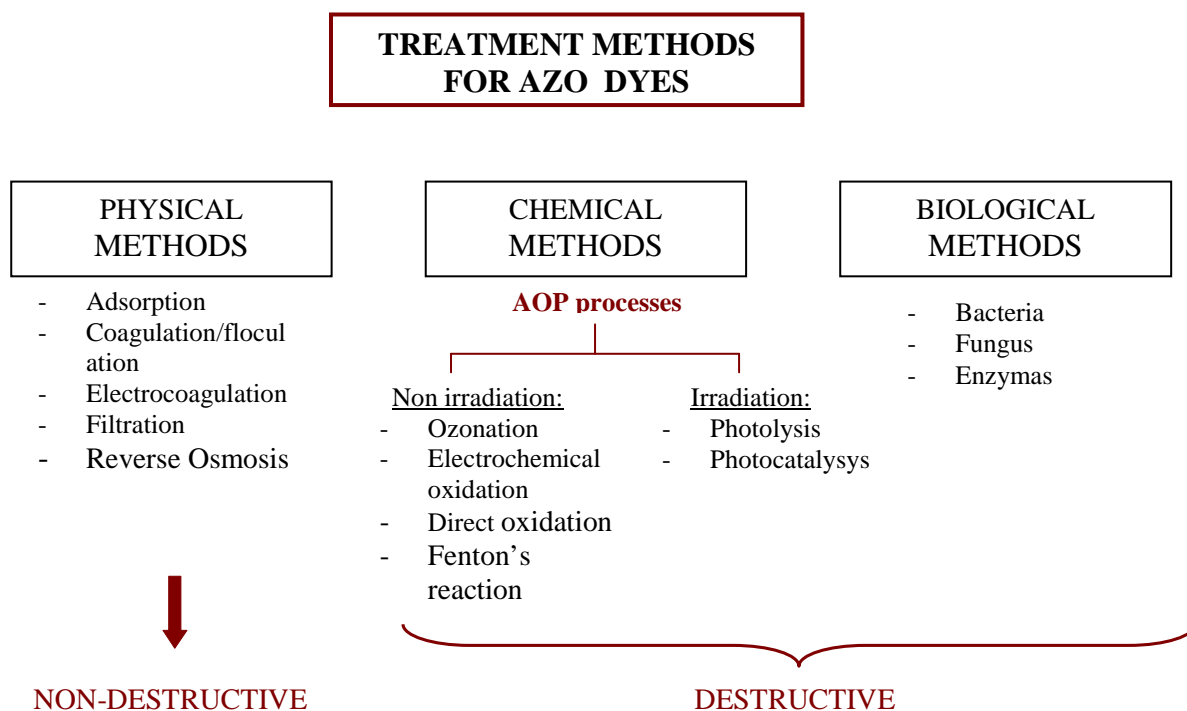NON-DESTRUCTIVE   DESTRUCTIVE

Fig. 2.7 Treatment methods for the removal of dyes from wastewater effluents.

2.2.1   Physicochemical technologies and biodegradation

2.2.1.1 Brief summary on the main methodologies

Physical methods are based on different principles, including several precipitation methods (coagulation or electrocoagulation, flocculation, foam flotation, sedimentation), adsorption (on active carbon, biological sludge, silikagel), filtration and reverse osmosis.

Among these the adsorption is the most used methodology, employed with different kind of adsorbents, inorganic or organic. The firsts have been preferentially applied because of their good mechanical and chemical stability, high specific surface area and resistance to microbiological degradation. In the last years adsorption onto Activated Carbon (AC) has proven to be one of the most effective and reliable physicochemical treatment methodologies [19, 20]. In particular if it is combined with other techniques like biodegradation [21, 22]. However, as the preparation of carbon sorbents is generally energy consuming, making the commercially products fairly expensive, new absorbents have been found, such as coal, fly ash, silica and alumina. Also several organic supports, originated from renewable sources and waste or by-products of industrial processes without any commercial value, have been studied, such as: orange peel, waste banana pith, dead and pulverized macrofungus, etc. [13].

Filtration (that involves methods such as ultrafiltration, nanofiltration and reverse osmosis) could be a good methodology in water treatment and recycling processes, since it can reach high removal efficiencies. However to resolve the main problem of fouling and so improve the efficiency of membrane filtration a combination with physic-chemical techniques, such as coagulation or flocculation, has to be taken into account. Moreover both ultrafiltration and nanofiltration might be inefficient in reducing lower molecular weight dyes, requiring post treatments, and the results strongly depend on the type of the material constituting the membrane [18, 23].

Biological methods constitute another important group into the dye-removal techniques. In this case contaminants are removed from wastewaters by means of living organisms, such as: bacteria, fungus and enzymes. Generally the mechanism behind the

bioremediation is based on the action of the biotransformation azoreductase enzymes, such as laccase, lignin peroxidase, hexane oxidase, etc., which catalyse the reductive cleavage of highly electrophilic azo bond [24].

This reductive reaction is carried out under anaerobic conditions and represents the first step in the bacterial metabolism, in which hazardous aromatic amines of the dye related structure are formed. As these compounds are not degraded under anaerobic conditions and tend to accumulate to toxic levels, a second aerobic treatment is need in order to degraded amines into non aromatic intermediates [13, 15, 24]. In addition it was been studied that aromatic compounds carrying SO_3H group as substituents often resist biodegradation and are not degraded under anaerobic condition [15] For these reasons, although anaerobic reduction is generally more effective than aerobic degradation, several methodologies have been developed for the successive anaerobic/aerobic treatment of dyes wastewater, such as: reactors designed on a sequential change among anaerobic/aerobic conditions [16] or whole bacterial cells in which dyes are adsorbed onto the biomass [25].

Also fungi have proved to have a considerable biotechnological interest due to their high biodegradation capacity and to the relatively non-specific nature of their ligninolytic enzymes [24]. Specifically white-rot fungi (among all the most widely used is *Phanerochaete chrysosporium*) produce a wide variety of extracellular enzymes that decompose highly stable products, like dyes [13]. However, the application of white-rot fungi has some inherent drawbacks including the long growth cycle and the need for nitrogen limiting conditions [24].

The employment of enzyme preparations isolated from microorganisms has been extensively investigated, showing considerable benefits over the direct use of bacteria: they can be easily standardized, simply applied and rapidly modified according to the type of the dyes to be removed [13].

2.2.1.2 Advantages and drawbacks

In general the main advantage of physicochemical techniques is that they are very efficient with all kind of dyes. Their main drawbacks are: the high cost and the production of a secondary pollution. In fact these traditional methods are non-

destructive and mainly provide a phase transfer of the contaminants from wastewater to solid waste, requiring potentially expensive post-treatment to be removed or regenerated.

On the other hand biological process is probably the most inexpensive one and, in addition, with it the complete mineralization is reached without the release of toxic products. However it must consider that these techniques involve living organism and, therefore, drastic conditions cannot be present, limiting the application to most textile wastewaters. Moreover various dyes are resistant to microbiological attack due to their complex structure and xenobiotic properties, making necessary the research of new strains of bacteria or the adaptation of existing ones for the decomposition of dyes.

2.2.2 Advanced Oxidation Processes (AOPs)

2.2.2.1 General principles: the role of OH• in the AOPs' destructive approach

Advanced Oxidation Processes (AOPs) refer to a set of different methods leading to the generation and use of highly reactive species, e.g. hydroxyl radicals OH•, as primary oxidants for the treatment of contaminants in wastewater since the formation of secondary pollution [12, 26]. In particular OH• is involved in the degradation process because of its high standard potential (E°=+3.06 V), which allows the partial or complete mineralization of several organic chemicals, with the formation of final degradation products as CO_2, H_2O and N_2 [12]. OH• radical reacts non-selectively with organic matter, producing organic radicals, which are highly reactive and can undergo further oxidation (Eq. 2.2) [27].

$$OH• + dye \rightarrow H_2O + dye• \rightarrow further\ oxidation \qquad (2.2)$$
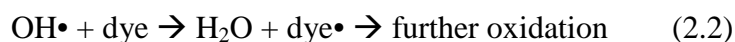
In this way decolorization and mineralization of dyes are achieved, producing inorganic compounds or, at least, transforming them into biodegradable or harmless products. Therefore, it is clear that they eliminate compounds rather than transferring into another medium such as a solid phase, in contrast with physical technologies [27].

Some of the AOPs are summarized in Table 2.3, in which the species and the conditions involved in each technique are indicated. Moreover, as shown in fig. 2.8, it is possible to distinguish between processes that doesn't need radiation and others that use radiation treatment with ultraviolet (UV) light [12, 17].

Table 2.3 Advanced oxidation processes.

METHOD	SPECIES AND CONDITIONS INVOLVED	REACTIVE INTERMEDIATES
Direct photolysis	UV	OH·
Ozone treatment	O_3 or O_3/H_2O_2	OH·, $HO_2·/O_2^-·$, $O_3^-·$
Fenton processes	H_2O_2/Fe^{2+} or $H_2O_2/O_3/Fe^{2+}$ (acid media)	OH·, $HO_2·/O_2^-·$, $O_3^-·$
Photo-Fenton processes	H_2O_2/Fe^{2+} or $H_2O_2/O_3/Fe^{2+}$ using UV light in addition	OH·
Photo-induced oxidation	UV or UV/O_3, UV/H_2O_2 using e.g. low pressure Hg lamp	$O_2^-·$, $O_3^-·$
Photocatalytic treatment	UV/vis light using TiO2, ZnO, etc. as catalyst	OH·
Electrochemical oxidation	Using an anode of high potential	OH·

TION PROCESSES

Direct photolysis
Dye + hv → CO_2 + H_2O

UV-peroxide photolysis
H_2O_2 + hv → 2OH•

Photocatalysis
TiO_2 + hv → (e+h)
H + OH^- → 2OH•

Photo-Fenton reaction
$Fe(OH)^{2+}$ + hv → Fe^{2+} + OH•

AOPs

NON-IRRADIATION PROCESSES

Ozonation
O_3 + H_2O → OH• + O_2

Fenton reaction
Fe^{2+} + H_2O_2 → Fe^{3+} + OH•

Electrochemical oxidation
H_2O → OH• + H_+ + e_-
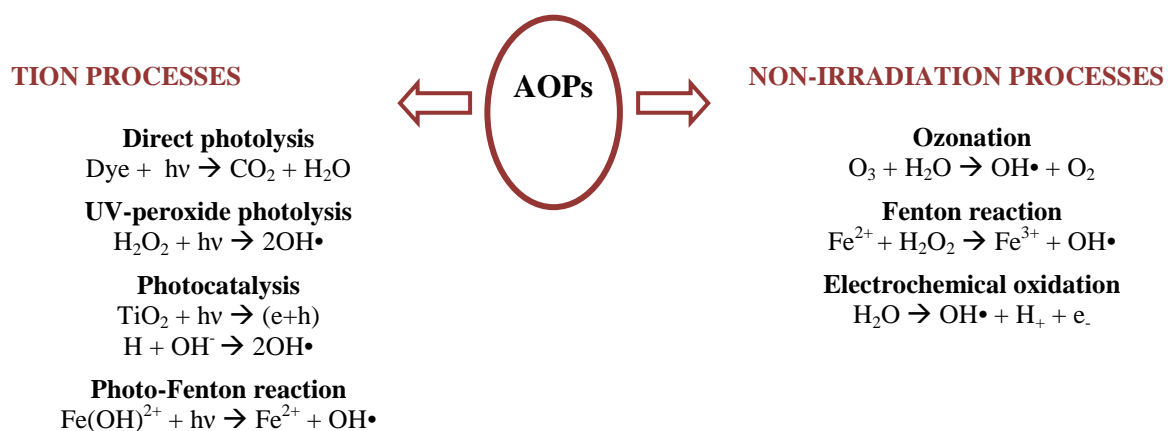
Fig. 2.8 Advanced oxidation Processes.

2.2.2.2 Direct irradiation and H_2O_2/UV photolysis

Among the irradiation processes, direct photolysis is the simplest and the most economic. It involves the interaction between organic molecules and the light in water solution, that leads to the break of bonds and, therefore, to the irreversible transformation of the matter (Eq. 2.3).

$$Dye + h\nu \rightarrow \ldots\ldots \rightarrow \rightarrow CO_2 + H_2O \qquad (2.3)$$

Although this technique is very cheap, it is not enough effective and a combination of light with other oxidizing agents, such as hydrogen peroxide (H_2O_2), ozon (O_3) or Fenton reagents, is needed [27].

The use of hydrogen peroxide in photolysis has been deeply studied in these last years. The mechanism most commonly accepted for the photolysis of H_2O_2, under UV radiation, is the cleavage of the molecule into hydroxyl radicals OH• (Eq. 2.4) [28]. Hydrogen peroxide can decompose also by a dismutation reaction (Eq. 2.5).

$$H_2O_2 + h\nu \rightarrow 2OH\bullet \qquad (2.4)$$
$$H_2O_2 + HO_2^- \rightarrow H_2O + O_2 + OH\bullet \qquad (2.5)$$
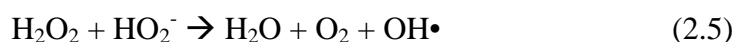
Mechanism of degradation of azo dyes in H_2O_2/UV photolysis

The reactions, that hydroxyl radicals can generate in presence of an organic substrate, may be differentiated by their mechanisms into three different classes: hydrogen abstraction, electron transfer and electrophilic addition [29, 30].

Hydrogen abstraction (Eq. 2.6) is the most common reaction through which hydroxyl radicals oxidize organic compounds. This reaction generates organic radicals that, by addition of molecular oxygen, yield organic peroxyl radicals (Eq. 2.7), initiating subsequent oxidation reactions, with the complete mineralization of the organic substrate.

$$OH\bullet + RH \rightarrow R\bullet + H_2O \qquad (2.6)$$
$$R\bullet + O_2 \rightarrow ROO\bullet \rightarrow \rightarrow \qquad (2.7)$$
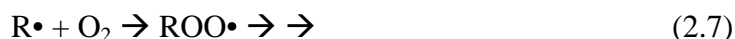
Electron-transfer reaction (Eq. 2.8) is of particular interest when hydrogen abstraction may be disfavoured by steric hindrance.

$$OH\bullet + RX \rightarrow RX^+\bullet + OH^- \qquad (2.8)$$

Hydroxyl radicals, produced upon photolysis, are electrophilic oxidants. Therefore oxidation of the dye may be initiated by the addition of OH• upon an electron-rich site, i.e. on the amino group (Eq. 2.9) or near the azo nitrogen atoms.

$$OH• + PhX \rightarrow HOPhX• \hspace{3cm} (2.9)$$
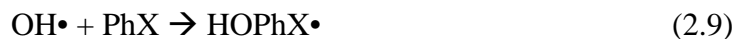
It has been proposed that oxidation of aminoazobenzene dye proceeds by the addition of an hydroxyl radical to the carbon atom bearing the azo bond, followed by the breaking of the resulting adduct [30].

Furthermore radical-radical recombination, that leads again to H_2O_2, must be taken into account (Eq. 2.10).

$$2OH• \rightarrow H_2O_2 \hspace{3cm} (2.10)$$

The reactions described represent the base for a correct interpretation of an azo dyes-degradation process carried out with photolysis. However, although many mechanisms have been proposed for the dye oxidation [12, 30], it should be noted that any case is different and depends on the characteristics of the dye molecule: the molecular structure, what kind of substituents are presented, steric hindrance, etc. For example the presence of sulphonate groups inhibits reactivity of the ring which carries them, as far as an electrophilic addition is concerned; consequently it can suppose that if in a dye molecule there is a benzene ring without sulphonate group, it may be the first target of hydroxyl radicals.

During the oxidation of a dye, aliphatic intermediates have been detected and, moreover, the inorganic anion SO_4^{2-} and carbon dioxide, CO_2, should be progressively formed.

Influential factors in the H_2O_2/UV photolysis

It has been established by several studies [26-28, 31, 32] that the efficiency of the degradation depends on the synergetic influence of several factors: the initial concentration of the dye, the initial concentration of H_2O_2, pH-value and the presence of inorganic ions.

H$_2$O$_2$ concentration seems to be the most influential factor. Because of the low molar absorption of H$_2$O$_2$ theoretically an excess of it is needed to produce more OH• radicals and experimentally it has been seen that removal rates are considerably increased by increasing the concentration of H$_2$O$_2$ [28]. However, further increase in the initial H$_2$O$_2$ may either enhance or inhibit the H$_2$O$_2$/UV process performance. In fact if an excess of H$_2$O$_2$ is used the equation 2.10 is promoted, favouring the production of hydroperoxyl radicals (Eq. 2.11) which are much less reactive and not contribute to the oxidative degradation of organic substrate [26, 29, 30].

$$H_2O_2 + OH• \rightarrow HO_2• + H_2O \qquad\qquad (2.11)$$

Therefore an optimum concentration of H$_2$O$_2$ must be used in order to maximize the photooxidation rate and then to make the process cost-effective.

Another important parameter is constituted by the initial concentration of the dye. Highly absorbing solutions, such as dyes, could act as filters limiting the penetration of light through the solution. In some studies it has been observed that a significant decrease of decoloration rate resulted at high concentration of dye. In fact in this last case most of the UV light will be absorbed by the dye molecules instead of the H$_2$O$_2$, decreasing the generation of OH• [26].

Finally the pH value seems not to be a determinant factor, above all in the case of mix solutions formed by several dyes, in which it is more important to focus on the interaction between the different compounds [31].

2.2.2.3 Other AOPs techniques

Besides photolysis other different techniques were developed for the degradation of organic pollutants in wastewaters. Among these there are: ozonation, Fenton and photo-Fenton reaction, and photocatalysis.

Since the ozone, O$_3$, was used for many years in order to decontaminate drinking water and for treatment of strongly contaminated residual water, its potential in conjunction with UV light as a method of removal organic material has been technically developed [29]. In the ozonation processes ozone reacts with organic compounds

dissolved in water through either direct ozone attack (Eq. 2.12) or indirect free radical attack (Eq. 2.12-2.14) [28].

$$O_3 + dye \rightarrow dye_{oxid} \qquad\qquad (2.12)$$
$$O_3 + H_2O \rightarrow OH\bullet + O_2 \qquad\qquad (2.13)$$
$$OH\bullet + dye \rightarrow dye_{oxid} \qquad\qquad (2.14)$$
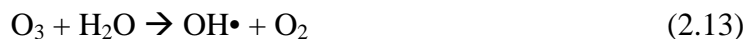
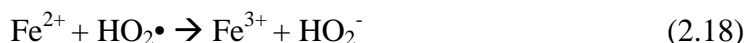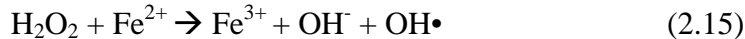The term Fenton reaction is referred to the oxidation of organic substrates by Fe^{2+} and H_2O_2. It was first described by H.J.H. Fenton who observed the oxidation of tartaric acid by H_2O_2 in the presence of ferrous iron ions. Although it has been known for more than a century, its application as an oxidizing process for destroying hazardous organics was not applied until the late 1960s [33].

In the classical Fenton reaction, the hydroxyl radicals are generated from the H_2O_2 reaction with Fe^{2+} ion (Eq. 2.15). Really after Fenton, others have postulated different mechanisms. One of these involves the production of free radical OH• that, adding to carbon bonds, can initiate a free radical mechanism, following the reactions:

$$H_2O_2 + Fe^{2+} \rightarrow Fe^{3+} + OH^- + OH\bullet \qquad\qquad (2.15)$$
$$OH\bullet + H_2O_2 \rightarrow HO_2\bullet + H_2O \qquad\qquad (2.16)$$
$$Fe^{3+} + HO_2\bullet \rightarrow Fe^{2+} + H^+ + O_2 \qquad\qquad (2.17)$$
$$Fe^{2+} + HO_2\bullet \rightarrow Fe^{3+} + HO_2^- \qquad\qquad (2.18)$$
$$Fe^{2+} + OH\bullet \rightarrow Fe^{3+} + OH^- \qquad\qquad (2.19)$$

There is still a controversy about the true mechanisms of Fenton reaction in solution, since several intermediates are formed during the process, and because the complexity of it.

When the degradation process is accelerated by a combination between UV radiation and iron salts, a photo-Fenton reaction takes place. The light has a positive role, since it stimulates the reduction of Fe^{3+}, previously formed in the reaction 2.15, to Fe^{2+} (Eq. 2.20); this last can react with H_2O_2, increasing the production of OH• radicals.

$$Fe(OH)^{2+} + h\nu \rightarrow Fe^{2+} + OH\bullet \qquad\qquad (2.20)$$
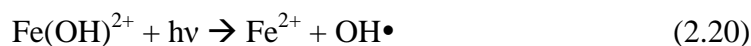
The photocatalytic processes are maybe the most investigated and widely used AOPs of the last past years [30, 34]. They include heterogeneous systems such as combination of semiconductors (MO/MO_2) and light, and semiconductor, light and oxidants. In these processes the photocatalysed decolorization of a dye in solution is initiated by the photoexcitation of the semiconductor, followed by the formation of electron-hole pair on the surface of catalyst (Eq. 2.21), placed on the conduction band (CB) and on the valence band (VB) respectively. The high oxidative potential of the positive hole (h^+_{VB}) permits the direct oxidation of the dye to reactive intermediates (Eq. 2.22).

$$(MO/MO_2) + h\nu \rightarrow (MO/MO_2)(e^-_{CB} + h^+_{VB}) \qquad (2.21)$$

$$h^+_{VB} + dye \rightarrow dye\bullet^+ \rightarrow oxidation\ of\ the\ dye \qquad (2.22)$$
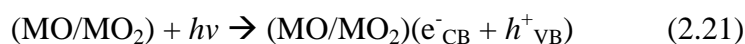
Also the hydroxyl radical is involved in the degradation process because of its high standard potential ($E°=+3.06$ V), which leads to the partial or complete mineralization as already mentioned (Eq. 2.23).

$$OH\bullet \quad + dye \rightarrow degradation\ of\ dye \qquad (2.23)$$
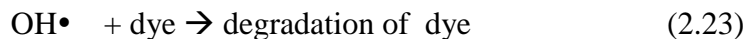
The radical $OH\bullet$ is formed either by the decomposition of water or by reaction of the hole with OH^- (Eq. 2.24-2.25).

$$h^+_{VB} + H_2O_{ads} \rightarrow H^+ + OH\bullet \qquad (2.24)$$

$$h^+_{VB} + OH^-_{ads} \rightarrow OH\ \bullet \qquad (2.25)$$

Titanium dioxide, TiO_2, was generally considered to be the best photocatalyst since it has the ability to detoxificate water from a number of organic pollutants. On the other hand it has been demonstrated [34] that ZnO is a more efficient catalyst and more economic than TiO_2. The main advantage of ZnO is that it absorbs over a larger fraction of solar spectrum than TiO_2 and, for this reason, it is the most suitable for photocatalytic degradation in the presence of sunlight.

2.2.2.4 Advantages and drawbacks

AOPs present inherent advantages, causing them to remain the most applied processes for the treatment of wastewater. Firstly, they are cleaner, because no sludge or secondary pollution are generated and dyes are totally decomposed to low-molecular-weight compounds CO_2 and H_2O. In addition they involve a minimal capital investment and an easy and fast operation procedure, with an high efficiency in the oxidation.

On the other hand they can be economically unfeasible, because of the elevate energetic costs. In order to overcome this problem it is possible improve them with some possibilities such as: constructing reactors that can use sunlight as a source of irradiation, using new materials or catalyst (in particular in these years nanocatalysts are widely studied), using inert surfaces in which the photocatalyst can be immobilized to favor its recovery or trying to improve the efficiency of degradation with different combination of processes.

Besides of this, efforts are being made to develop new technologies, such as electrochemical oxidation [2], that would be versatile, energy and cost effective, and easy to use.

2.3   ANALYTIC TECHNIQUES

In this section the analytic techniques used during the experiments are considered, focusing on their theorical basis and their common applications in dye detection and dye removal.

2.3.1   UV-visible spectroscopy

When a beam of light with an initial intensity I_0 strikes a compound, this can absorb part of the radiation, with the consequent decrease of the radiation intensity, from I_0 to I, and the excitation of the molecular ground states in the sample, causing electronic, vibrational and rotational transition. The amount of the radiation absorbed is quantitatively defined by *absorbance*, *A*, expressed as:

$$A = \log \frac{I_0}{I} \qquad (2.26)$$

An UV-visible spectrum is obtained by measuring the *absorbance*, *A*, of radiation belonging to the UV-visible spectral region (200-780 nm), passed through a sample normally located in a cuvette. Since the absorption of a radiation is dependent on the electronic structure of the absorbing compound, each chemical species will be characterized by a specific UV-vis spectrum, in which *A* is plotted as a function of wavelengths, λ, of the incident radiation.

As established by Lambert Beer's law (Eq. 2.27), *A* has a linear relationship with the concentration of the absorbing molecular species (C_m) and with the path length (l) which the light has to travel.

$$A = \varepsilon C_m l \qquad (2.27)$$

where ε is the *molar absorptivity*, constant for a particular chemical compound [35].

2.3.1.1 Absorption of organic compounds

In organic compounds the absorption of UV-vis radiation is due to the presence of functional groups, called *chromophores*, that possess valence electrons, with a low energy of activation, that can be readily promoted by the absorption of UV and visible light. The UV-vis spectrum of a molecule containing chromophore groups is rather complex because of the overlapping of vibrational and rotational transitions, so that the spectrum appears as a continuous line of absorption [36].

In particular for an organic compound the transitions, that can be achieved by the energies available on the 200 to 780 nm region, are $n \rightarrow \pi^*$ and $\pi \rightarrow \pi^*$. The firsts are observed in molecules containing lone pairs or nonbonding electrons and require energies lower than that for $\pi \rightarrow \pi^*$ transitions, resulting in the absorption in the UV-vis region. The $\pi \rightarrow \pi^*$ transitions characterize molecules containing π electrons and occur at wavelengths near ultraviolet regions. The conjugation of unsaturated groups further increases λ_{max}.

The effect of conjugation is quite important in aromatic compounds, which present several absorption bands in the UV region. The E (Ethylenic) and B (Benzenoid) bands are relative to $\pi \rightarrow \pi^*$ transitions and they absorb at 180-200 nm and 250-255 nm, respectively. These band are common for all the molecules containing a benzene ring. When the ring is bounded with an unsaturated group, capable to conjugate with it, as in the case of a chromophore, K band (Conjugation band) appears. Instead, the presence of a substituent group with lone pair of electrons, like a auxochromes, determines a $n \rightarrow \pi^*$ transition and a R band (Group Type band) is observed (Tab.2.4), with a consequent increase of λ_{max} and absorption to higher wavelengths of the visible region.

Tab. 2.4 Increase of λ_{max} of some compound due to increase of conjugation.

COMPOUND	λ_{max} K BAND	λ_{max} B BAND	λ_{max} R BAND
Benzene		255	
Styrene	244	282	
Benzaldehyde	244	280	328
Nitrobenzene	252	280	330

2.3.1.2 Spectrophotometer with diode array detector

In fig. 2.9 is shown the basic scheme of a spectrophotometer with diode array detector, as it is the instrument used in this study.

The principal characteristic of a diode array UV-vis instrument is that data for many wavelengths can be acquired simultaneously thanks to the presence of hundred or thousand detectors (from 128 to 1024 silicon-diodes and even up to 4096) packed close together. These arrays of detectors record the signal simultaneously over the whole spectral region. In this way an instantaneous spectral acquisition can be reached, making diode array spectrophotometer an important instrument for measurement of fast chemical reactions and for kinetic studies; this property is called the *multichannel advantage* of multidetector systems [37].

This advantage is a consequence of the instrumental configuration. The beam light source is focused directly on the sample, so that radiations of all the wavelengths strike the sample at same time. The radiation, coming out of the sample after absorption, is then directed on a reflection grating, that reflects the beam and disperses all the wavelengths simultaneously to the diode array detector.
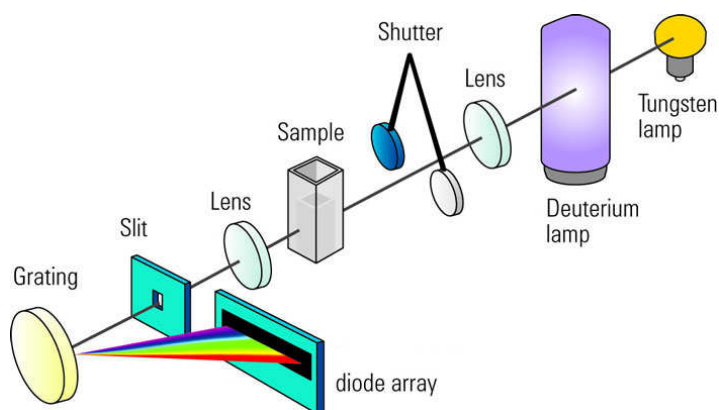

Fig. 2.9 Scheme of a UV-Visible spectrophotometer with diode array detector.

2.3.1.3 Application in dye detection and dye degradation monitoring

UV-visible spectroscopy has proved to be an useful tool for both dye detection and the monitoring of dye degradation process.

Since azo dyes are organic compounds composed by benzene rings and functional groups like -N=N-, as chromophores, and other auxochromes, they are characterized by an elevated electron delocalization, that makes them naturally colored compounds. It follows that the visible spectral region is appropriate for qualitative and quantitative analysis of azo dyes.

In addition during a degradation process of an azo dye, it is possible to obtain information about the intermediates produced using the UV range. In a classical approximation the monitoring of the process is normally carried out observing the wavelength of maximum absorbance or, exactly, of the two main absorption bands (E and B bands). Decreases in absorbance at these wavelengths correspond to loss of aromaticity of the dye, that degrades into low-molecular-weight compounds. With this information is possible to calculate the *decolorization efficiency (%)* (Eq. 2.27), that may be considered as a quantify parameter for monitoring the degradation process.

$$efficiency(\%) = \frac{A_0 - A}{A_0} \times 100 \qquad (2.27)$$

where A_0 is the initial absorbance of the dye and A is the absorbance of dye after the process [34].

It is clear that UV-vis spectrophotometric determination permits to obtain rapid response using a relatively simple procedure, with low experimental costs and short analysis time. However the lack of selectivity, that characterized this technique, can lead to erroneous results if there is more than one dye or interferences in the reaction medium, or formation of byproducts, that absorb at the same wavelength of the dye. Therefore, UV-vis spectroscopy must be coupled with other techniques as chemometric treatments of multivariate data, which allows quantification of analytes in presence of interferences [3, 32, 38, 39].

2.3.2   Mass spectrometry

Mass spectrometry is a powerful tool in analytical chemistry that provides detailed structural information on a wide variety of compounds with molecular weight of 1-1,000,000 Da by using a small amount of sample. It is based on the generation of gaseous ions from analyte molecules, the subsequent separation of the ions according to their mass-to-charge ratio, *m/z*, and the detection of these ions [40, 41].

The resulting mass spectrum is a plot of the abundance of the ions produced as a function of the *m/z* ratio. The signal, relative to the abundance, is usually called *peak*, and the distance between peaks represents a loss from the ion at higher m/z to produce the fragment ion at lower m/z.

In particular two peaks are relevant in a mass spectrum: the *molecular ion peak* and the *base peak*. The first results from the detection of the intact ionized molecule, the *molecular ion*, $M^{+\bullet}$, and usually it is the peak at highest m/z. The second is the most intense peak of a mass spectrum and normally its intensity is normalized to 100% relative intensity in order to determine the relative abundance of the other peaks.

2.3.2.1 Mass Spectrometry with Electrospray Ionization source (ESI)

In fig. 2.10 is depicted the general block diagram of a mass spectrometer. Normally it consists of five parts: sample introduction, analyte ionization, mass separation, ion detection and data handling.

In general a mass spectrometer can be coupled with gas chromatographic technique (GC) or with liquid chromatographic technique (LC). In this last case the interface between the two different instruments plays a very relevant role, since it must connect an atmospheric-pressure system with a vacuum one [35]. This problem has largely been solved by the advent of new soft ionization techniques, such as Electrospray Ionization (ESI), that can be considered as an inlet system to the mass spectrometer and an ion source at the same time.
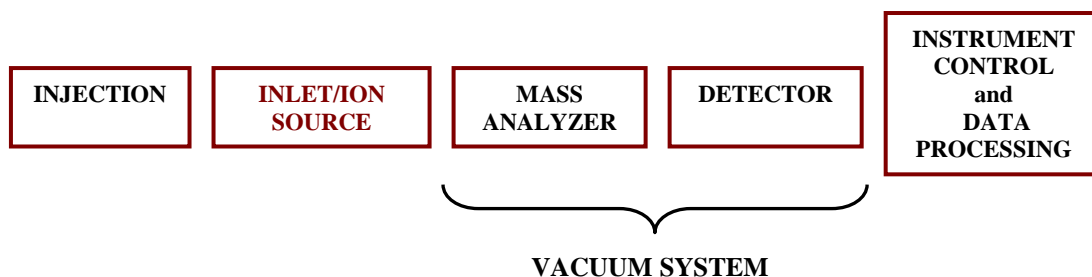
Fig. 2.10 Block diagram of a mass spectrometer with ESI inlet/ion-source ESI

.

The ESI interface is an Atmospheric Pressure Ionization interface (API), since it accomplishes the transfer of ions from solution to the gas phase through the nebulization of a liquid stream into an aerosol of highly charged droplets and enables the ionization of the analyte after desolvation of the droplets produced.

In fig 2.11 is shown a scheme of an ESI interface. Previously the analyte is introduced into the ESI source via a needle either by direct injection or as an eluent flow.
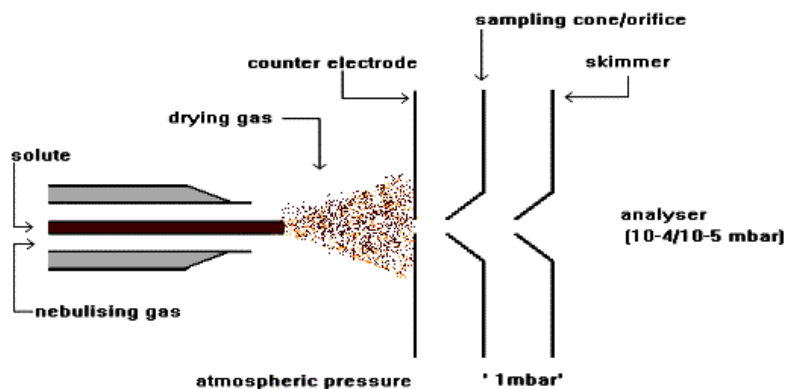

Fig. 2.11 Scheme of the ESI inlet/ion-source.

Then the solution is passed along a short length of stainless steel capillary tube, to the end of which is applied a high positive or negative electric potential (3-5kV), that charges the surface of the liquid emerging from the needle, creating a fine spray of charged droplets. Driven by the electric field, the droplets pass through a curtain of nitrogen drying gas, which supports evaporation of the solvent and also prevents the uncharged material from entering the ion source. By expansion of the curtain gas, the

ions are carried through two evacuated regions via a nozzle and a skimmer, two conically shaped hole, and finally into the analyser of the mass spectrometer [42].

ESI is a soft ionization technique that results in little fragmentation and thus provides molecular mass information. It is extremely useful for accurate mass measurement, particularly for thermally labile, high-molecular-mass substances.

2.3.2.2 Application in identifying reaction intermediates and dye degradation mechanism

Several analytical techniques can be employed in order to determine the degradation pathway, the intermediates and the final products of the dye-degradation process. Among these MS offers a sensitive and specific detection with reliable identification of analytes, especially in the case of complex sample matrix.

In general the classical GC-MS with Electron Impact (EI) source is often the first technique chosen, since it can be used with a variety of compounds. Nonetheless, under the conditions set up for this method, polar organic compounds, like dyes, are not volatile and are destroyed thermally in the injector because of their poor thermal stability. Furthermore the EI source yields an high fragmentation, that can prevent the obtaining of molecular mass in less stable compounds [43, 44].

Instead, the employment of soft ionization sources, such as ESI, allows to analyse non-volatile ionic and polar dyes and identify abundant intermediates better, since it causes minimal fragmentation. For this reason in the last years ESI, in positive- and negative ion mode, has been widely applied for the detection of dyes and their degradation products.

2.4 CHEMOMETRIC METHODS

2.4.1 Introduction: definition of chemometric and data orders

The development of the chemometric analysis was a natural and necessary consequence of the rapid evolution of instrumental analytical chemistry, that led to the problem of the evaluation and interpretation of a vast amount analytical data [35]. Chemometric, with the application of mathematical and statistical, overcomes this problem and allows "to design or select optimal experimental procedure; to provide maximum relevant chemical information by analysing chemical data; and to obtain knowledge about chemical systems" [45].

Experimental measurements generated by analytical instruments can be classified in *univariate* or *multivariate data*. The data of the first group, also called *zero-order data*, are obtained when one variable is measured for each samples. In this case there is one scalar per sample (e.g. an absorbance at one wavelength). The multivariate data are generally *first-order data*, when there is one vector per sample (e.g. an absorbance over time) and *second-order data*, when there is one matrix per sample (e.g. a spectrum over time). When the order of the data increases, the complexity of the mathematical/statistical data processing also increases.

2.4.1.1 Chemometric analysis of evolving second-order data

Experimental data, related to a system evolving in function of a variable increasing or decreasing (e.g. time or pH), are called second-order data. An example is given by the data collected with a UV-visible spectrometer in function of the time, that can be arranged yelding a matrix **D** (*m* x *n*) (fig.2.12), in which rows represent the *m* spectra detected at each *m* time and columns gives the *n* wavelengths of measure.

These kind of matrices, obtained from the measure of second-order data in function of an evolving variable, can be treated with the methodology of Multivariate Curve Resolution-Alternating Least Square (MCR-ALS) [46, 47].
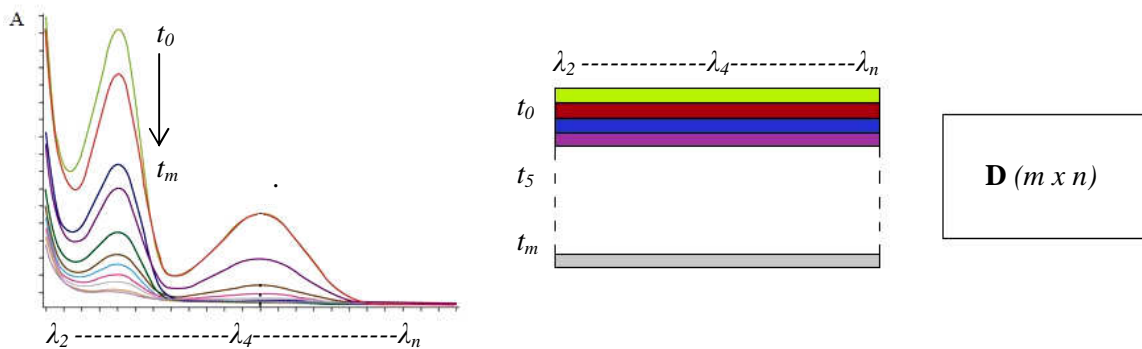

Fig. 2.12 Matrix of second order data.

2.4.2 Multivariate Curve Resolution with Alternating Least Square (MCR-ALS)

MCR-ALS decomposes a data matrix into the product of two matrices (fig. 2.13), assuming that the experimental data follow a linear model:

$$\mathbf{D} = \mathbf{C}\mathbf{S}^{\mathrm{T}} + \mathbf{E} \qquad\qquad (2.28)$$

when the experimental data in the matrix **D**, containing the series of the spectra collected at different values of a certain variable (e.g. time), can be expressed as the product of two matrix, **C** e $\mathbf{S}^{\mathrm{T}}$, which contains the concentrations profiles of each

chemical species as a function of the process variable and the related pure spectra of those species, respectively. **E** is the matrix of residuals, that contains the variability not explain by the model and ideally should be close to the experimental error. The dimensions of these matrices are **D** (*m* x *n*), **C** (*m* x *p*), **S**^{T} (*p* x *n*) and **E** *(m* x *n)*, whit *m* the number of spectra analysed, *n* the number of spectroscopy wavelengths recorded for each spectrum and *p* the number of components involved in the process.
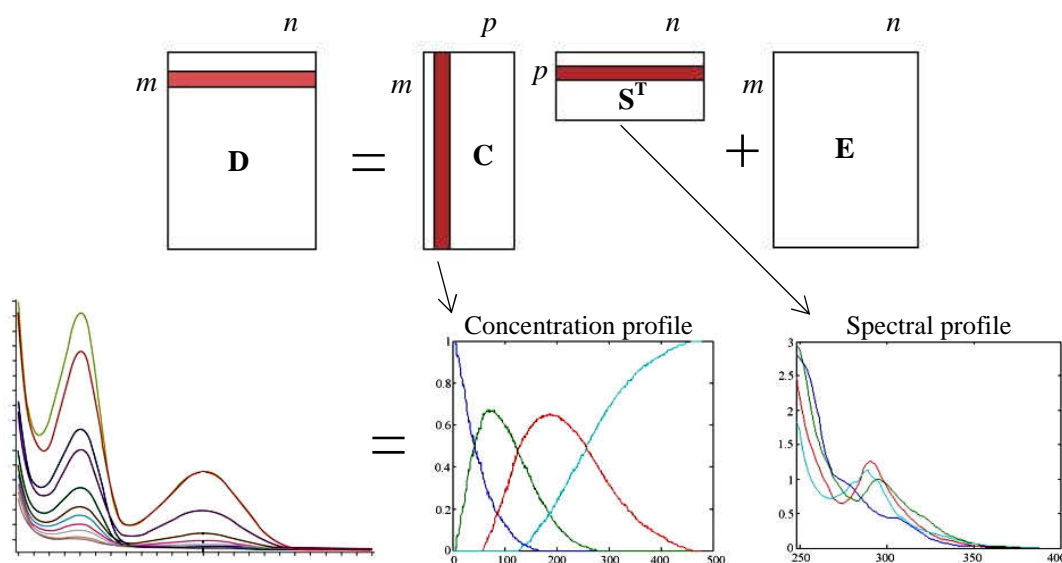

Fig. 2. 13 MCR-ALS applied to the decomposition of matrix D.

MCR-ALS analyses the matrix **D** as a iterative resolution method, in which at each iterative cycle of the optimisation process, matrices **C** and **S**^{T} are calculated under constraints so that they minimise as much as possible the error in the reproduction of the original data set **D**, in order to obtain a solution with chemical meaning. Generally, MCR-ALS is performed following several and fundamental steps (fig. 2.14):

1. Evaluation of the number of components *p* that make a significant contribution to the signal response and that are related to the number of chemical species presented in the studied system. This first step can be carried out with Components Analysis (PCA) by Singular Value Decomposition, or other algorithms, that express the relevant information contained in a data matrix **D** (*m*

$\times$ *n*) in a reduced number of hierarchized variables known as principal components.

2. Search for matrices of the initial estimations of **C** (concentration profiles) or **S** (spectral profiles). For this purpose Evolving Factor Analysis (EFA) is used.

3. Finally, the alternative least-squares (ALS) algorithm is applied to obtain the spectral and the concentration profiles of the species involved in the process. In this last step some constrains can be applied to drive the final solution towards a chemical meaning.
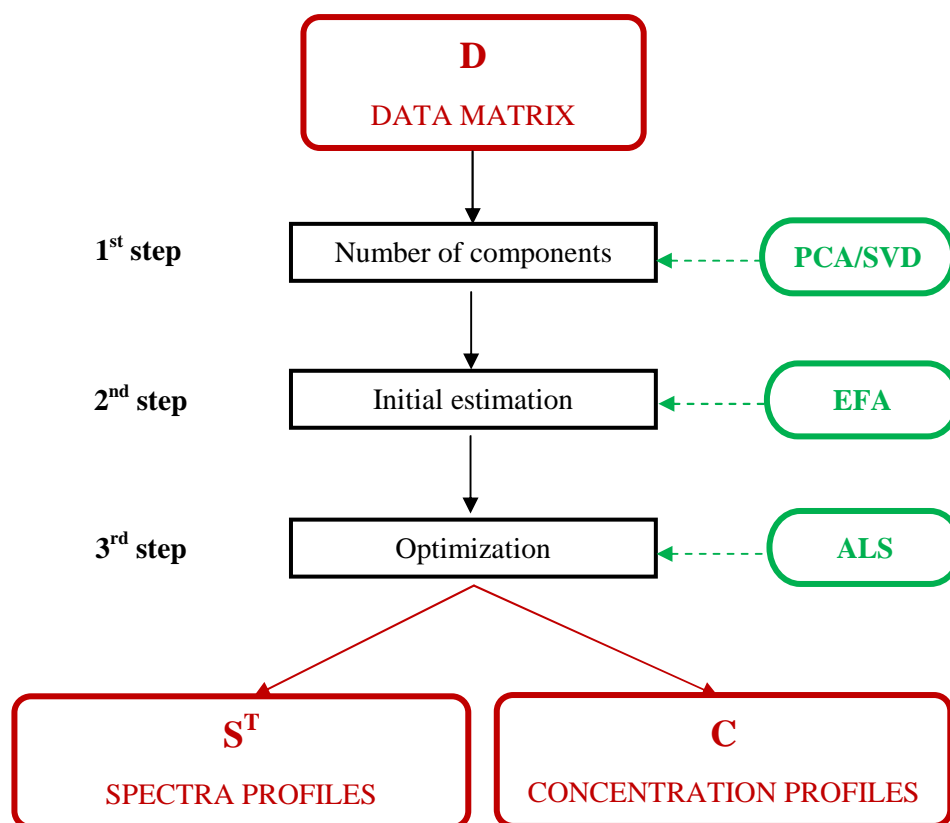

Fig. 2.14 Scheme of the resolution process of the MCR-ALS method.

2.4.3 Evaluation of the number of components by Singular Value Decomposition (SVD)

The evaluation of the number of components involved in the process studied is a fundamental point to carry out an analysis of curve resolution, because of the number of components is related to the number of real causes of variation [48].

This aim can be reached with different methodologies like PCA (Principal Component Analysis), SVD (Singular Value Decomposition) and EFA (Evolving Factor Analysis). As in the work here presented, the SVD has been used for this purpose, only this will be explained in this paragraph.

In an SVD analysis the matrix $\mathbf{D}$ (m x n) is decomposed in three matrix $\mathbf{U}$ (m x m), $\mathbf{W}$ (m x n) and $\mathbf{V}$ (n x n), in this form:

$$\mathbf{D} = \mathbf{UWV}^{\mathrm{T}} \tag{2.34}$$

where $\mathbf{U}$ and $\mathbf{V}$ are column-orthonormal matrix related to the scores of the objects and to the loadings of variable respectively. $\mathbf{W}$ is a diagonal matrix that contained the singular values, arranged in ascending order, describing the amount of variance presents in each component [45].

In order to determine how many meaningful components should be retained, different approaches can be applied: empirical, such as the interpretation of a scree plot; statistical, for example by means of the F-test; or by internal validation, like the cross-validation method [49].

2.4.4 Search for initial estimations with Evolving Factor Analysis (EFA)

When the number of components has been determined, it can be used to obtain the initial estimations of the both profiles, concentration $\mathbf{C}$ and spectral $\mathbf{S}^{\mathrm{T}}$. There are several mathematic methodologies that can be used to achieve this purpose, like Evolving Factor Analysis (EFA) [48, 50, 51].

EFA examines the evolution of the rank of a matrix of data by systematically subjecting submatrices of the complete data matrix to factor analysis.

The process, shown in fig. 2.15, starts from the first row of the data matrix, e.g. the first spectrum measured, for which singular values are calculated. Afterwards a second row is added and SVD is performed on two rows, and so on for the whole matrix **D**. As this process evolves forward on the ordered variable, it is known as *forward* EFA (*f*E). When EFA is performed in the opposite direction, analysing an increasing number of rows, beginning from the end, the so called *backward* EFA (*b*E) is obtained.
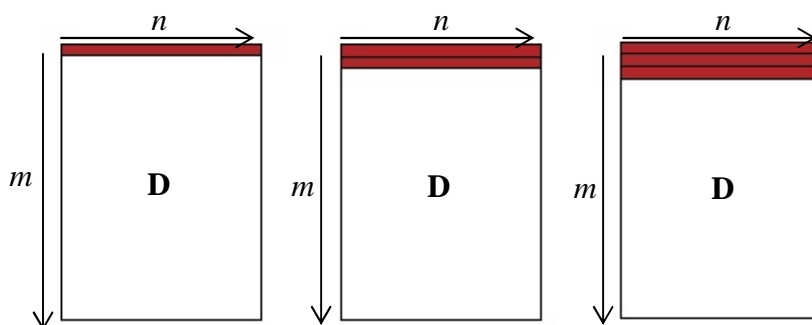

Fig. 2.15 Process of forward EFA. The shaded areas represent the submatrices (rows) on which SVD is performed.

Normally an EFA plot results by combination of *fE* and *bE*, plotting the logarithms of the singular values recorded against the ordered variable. As example, in fig. 2.16 the EFA plot for a real case is proposed. In this example a matrix with 61 rows and 40 columns is analysed. Observing the plot several information can be yielded:

- the noise level;

- in the *f*E the appearance of each components is observed, since the number of singular values above the noise level equals the number of the underlying species (three in the case given, represented by lines *f*1, *f*2 and *f*3);

- in the same way, the *b*E shows the disappearance of each component (represented by lines *b*1, *b*2 and *b*3) from the system.

Therefore an EFA plot gives information about the number of the components, which have a significant signal compared to the noise, and their region of existence, also called *concentration region*, without making any particular assumptions.
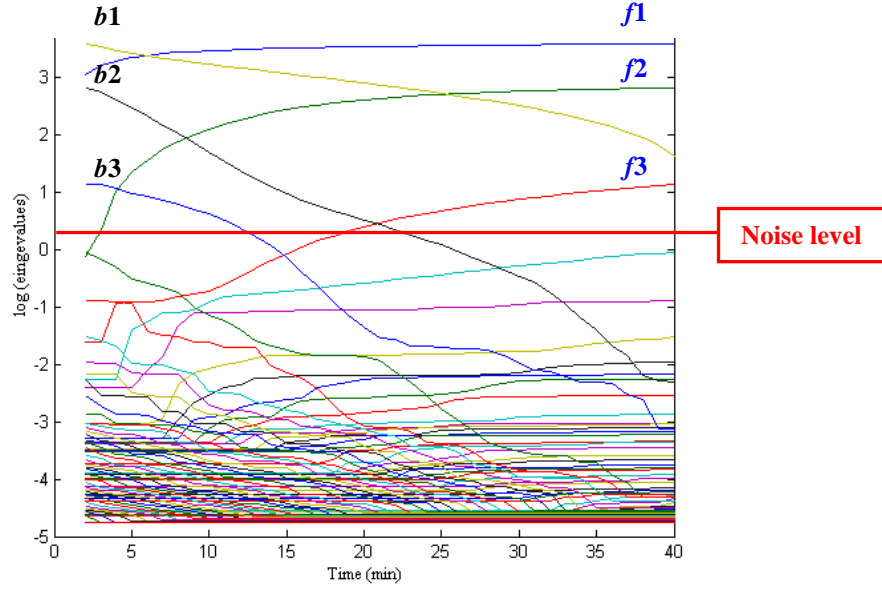
**Fig. 2.16 EFA plot obtained analysing a matrix,
yielded from a real case of study with dimensionality (61 x 40).**

2.4.5   Optimization with Alternative Least Square (ALS) algorithm

After obtaining the initial estimates of $\mathbf{S}^T$ and $\mathbf{C}$, these are optimized by solving iteratively the alternative least-squares (ALS) algorithm (Eq. 2.29–2.30). At each iteration of the optimization a new estimation of the $\mathbf{C}$ and S matrices is obtained.

$$\mathbf{S}^T = \mathbf{C}^+\mathbf{D}* = \mathbf{C}^+\mathbf{C}\mathbf{S}^T \qquad\qquad (2.29)$$

$$\mathbf{C} = \mathbf{D}*(\mathbf{S}^T)^+ = \mathbf{C}(\mathbf{S}^T)(\mathbf{S}^T)^+ \qquad\qquad (2.30)$$

where matrix $\mathbf{D}*$ is the experimental data matrix reconstructed for the selected number of components, $(\mathbf{S}^T)^+$ and $(\mathbf{C})^+$ are the pseudo-inverse of the $\mathbf{S}^T$ and $\mathbf{C}$ matrices, respectively [46].

The iteration procedure is stopped when convergence is achieved or when a preselected number of cycles is reached. The attainment of convergence occurs when, in two consecutive iterative cycles, relative differences between the residual of one iteration and the next is less than a previously selected value (usually chosen at 0.1%) [52].

2.4.5.1 The role of constraints

Although multivariate resolution doesn't require previous knowledge about the chemical system under study, additional knowledge can be used to improve the results obtained. This is the role of constrains, that force the iterative optimization process to model the profiles respecting the condition desired.

A constrain can be defined as any mathematical or chemical property systematically fulfilled by the whole system or by some of its pure contributions [53].

Most of the constraints are directly linked to chemical properties fulfilled by the pure concentration or response profiles. Among these there are: non-negativity, unimodality, closure and selectivity [46, 48, 52]. The first is the most general constraint and it is used to force the concentration or spectral profile to be positive. This restriction is applied easily to spectrophotometric systems, in which it is supposed that the spectral profiles have always positive values of absorbance. Unimodality is applied for the profiles which is presumed to have only one maximum, therefore it is frequently used in concentration profiles and not much with spectral ones. Closure was valid in many reacting systems in which the amount of the matter is constant. Selectivity holds for concentration and spectral window where only one component is present.

Because of the mathematical simplicity of the algorithm, constraints can be used in a very flexible way. Thus, different constraints can be applied to the profiles in $\mathbf{C}$ and in $\mathbf{S}^T$ or to the different chemical species within each of these two matrices.

2.4.5.2 Parameters of quality

The parameters, normally used to evaluate the goodness of the optimization process, are: the percent of lack of fit and the percent of variance explained respect experimental data [48, 52].

Lack of fit, LOF, is defined as the difference between the input data matrix $\mathbf{D}$ and the matrix reproduced from the $\mathbf{CS}^T$ obtained by MCR-ALS. This value is calculated with the following expression:

$$lackoffit(\%) = \sqrt{\frac{\sum\limits_{i,j} e_{ij}^2}{\sum\limits_{i,j} d_{i,j}^2}} \tag{2.31}$$

where e_{ij}^2 is the related residual obtained from the difference between the input matrix and the matrix reconstructed by MCR-ALS, and d_{ij}^2 designs an element of the input data matrix.

Percent of variance explained, R^2 (Eq. 2.32) respect experimental data are calculated according to the equations:

$$R^2 = \frac{\sum\limits_{i,j} d_{i,j}^2 - \sum\limits_{i,j} e_{ij}^2}{\sum\limits_{i,j} d_{ij}^2} \tag{2.32}$$

where d_{ij}^2 and e_{ij}^2 are the same as above and n_{rows} and $n_{columns}$ are the numbers of rows and columns in **D**. Also the values of the residuals, decreasing with optimization, are adopted to evaluate the quality of the fitting.

In addition also the calculation of the correlation (r) between a pure known component and the result of the ALS process, could be used to evaluate the goodness of the optimization.

- 3 -

EXPERIMENTAL CONDITIONS

3.1 MATERIALS, INSTRUMENTS AND METHODS

3.1.1   Chemicals

The reagents used in this study were analytical grade chemicals. Acid Red 97 was obtained from Trumpler Española, S.A. (Barberà del Vallès, Barcelona, Spain) and H_2O_2 (30%) was purchased from Scharlau. All solutions were prepared with ultrapure Milli-Q water from a system supplied by Millipore (USA).

3.1.2   Instrumental and measuring conditions

3.1.2.1 Reactor

Photodegradation experiences were carried out in a cylindric batch reactor (fig. 3.1) formed of a Pyrex glass outer reactor with a capacity of 0.7 L and a quartz immersion tube (2.5 cm i.d. and 38 cm in length).
The reactor contains a low pressure mercury vapour lamp (LPML) of 15 W (Heraeus Noblelight, Germany). The light source emits at 254 nm and the incident photon flux of the   UV   reactor   is   0.1 Wcm^{-1}.
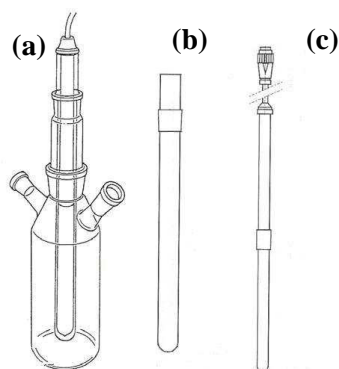
**Fig. 3.1 Scheme of the photoreactor used: cylindric reactor (a),
outer reactor (b) and quartz tube (c).**

3.1.2.2 UV-vis spectrophotometer

Spectral data were acquired using a diode-array spectrophotometer (Shimadzu MultiSpec-1501) and Hyper-UV 1.51 software. The UV-visible spectra of the dye and the blank degradation were recorded at each nm from 250 to 720.

3.1.2.3 Mass Spectrometer

MS spectra were obtained by direct injection on an 6210 LC/TOF mass spectrometer (Agilent Technologies, Palo Alto, U.S.A.), equipped with an electrospray ionisation source (ESI). MS source parameters were set with gas temperature of 250ºC, drying gas flow of 5 l/min, nebulizer gas pressure of 12 psi, and a capillary voltage of 3500 V. Data acquisition was realised in negative acquisition mode, with a skimmer voltage of 65V, a fragmentor voltatge of 150V, and an acquisition range from 50 to 1500 m/z, at a rate of 1.02 spectra/sec. The instrument was calibrated in negative ion modes using a tuning mixture (1:4 dilution in 95:5 Acetonitrile/water). Reference mass correction was carried out using ions at 119.036320 (purine, CAS No. 120-73-0) and 1033.988109 (hexakis(1H, 1H, 3H-tetrafluoropropoxy) phosphazine, CAS No. 58943-98-9), both from Agilent Technologies, Palo Alto, U.S.A.. The results were handled through Agilent Mass Hunter Qualitative Analysis software (version B.01.03).

3.1.3   Software

The UV-visible spectra recorded were exported and converted in MATLAB file, and the matrices obtained were analysed by MCR-ALS using MATLAB 7.0 computer environment [52].

3.2   PRELIMINARY EXPERIMENTAL STUDIES

Relying on the results of a previous study [31], several experiences were formerly carried out in order to determine the best experiment conditions for the degradation of dye A.R. 97. The aim of this preliminary study was to establish a method that allows to obtain a good degradation but in the meantime also an easy control of the process.

During these experiments different factors, that could influence degradation reaction (dye concentration, pH value and H_2O_2 concentration), were checked. In table 3.1 some of these experiments are provided, showing for each one the conditions used and brief considerations. It follows that a good degradation might be achieved with a dye concentration of 30 mg/L and with a pH value of 6.5, that is the pH of the dye.

In addition it derives that only the variation of H_2O_2 concentration have a decisive influence on the photooxidative degradation of dye A.R. 97. Therefore, it has decided to investigate more deeply the influence of H_2O_2 concentration on the rate of degradation process.

Table 3.1 Conditions and considerations of some preliminary experiments.

DYE (MG/L)	H_2O_2 (M)	PH	NOTES
50	No	6.5 (dye pH)	Slow degradation. Likely influence conditions: - dye concentration too high; - H_2O_2 concentration too low; - pH value too high.
50	0.05	2	Fast degradation. The process cannot be controlled. Likely influence conditions: - pH value too low.
50	0.02	6.5 (dye pH)	Good degradation trend, achieved using the dye pH value and a low H_2O_2 concentration.
30	0.02	6.5 (dye pH)	With a lower dye concentration the degradation process is simpler to control.

3.3 PHOTODEGRADATION PROCEDURE

3.3.1 Preparation of the solutions of dye A.R.97

During the study four different photodegradation experiences, indicated as Exp1, Exp2, Exp3 and Exp4, were carried out. For each experience a solution was prepared with 30 mg/L of dye A.R.97 in 0.5 L of milli-Q water.

As table 3.2 shows, only Exp1 was conducted without the presence of the oxidant, while for the other three experiment aliquots of increasing concentration of H_2O_2 were added.

Tab. 3.2 H_2O_2 concentration used for each experiment.

EXPERIMENTS	H_2O_2 (M)
Exp1	--
Exp2	0.02
Exp3	0.05
Exp4	0.1

3.3.2 Photodegradation process procedure

Once a solution was prepared, adding the necessary aliquot of H_2O_2 (in the case of Exp2, 3 and 4), it was introduced into the reactor, immediately turned on. The process was carried out at room temperature with continuous stirring for 60 minutes.

Six-millilitre samples of the degradation solution were taken, from the reactor using a syringe, at the beginning of the experiment (t=0) and after each minute throughout the degradation time. Each sample was analysed in the UV-vis spectrophotometer, so that, at the end of the process, a total of 61 spectra was recorded.

Afterwards, the degradation of H_2O_2, taken as blank, was carried out under the same conditions, in order to determine the background of the process.

3.4 DATA HANDLING WITH MCR-ALS

3.4.1   Parameters of optimization

For the iterative procedure of ALS algorithm the value of convergence criterion was fixed at 0.1% and the maximum number of iterations allowed at 500.

The following constrains have been applied: non negative for both concentration and spectral profiles and unimodality only for concentration profile.

The goodness of optimization was checked assessing:

- the LOF respect to the PCA (LOF % PCA);

- the explained variance (R^2);

- the correlation coefficient (r) between the spectrum of the pure dye and the resolution results.

3.5 MASS SPECTROMETRY ANALYSIS

Mass Spectrometry analysis was performed only for the experiment that allowed to determine more clearly the evolution of intermediate species during the process, since the aims of MS analysis were:

- to determine the possible chemical intermediates of degradation;
- to propose a reaction pathway of the process.

For this purpose the slower experiment was supposed to be the most suitable.

3.5.1 Samples collecting

Once determine the slowest experiment, specified times, in which collecting representative samples during the process, have been selected.

The determination of times have been conducted taking into account the information obtained from EFA analysis of spectra data matrices. In fact this method allows to detect the reaction times in which significant variation occurs, namely when a new component emerges.

Then the experiment was repeated collecting the samples at minutes selected and the samples were stored in the dark because of their photosensitivity.

3.6 EVALUATION OF INFLUENCE OF H_2O_2 CONCENTRATION

3.6.1 Determination of efficiency decolorization

To evaluate the influence of H_2O_2 concentration, firstly the *decolorization efficiency (%)* (Dec. Eff.) were determine for the four degradation processes. This parameter, introduced in the chapter 2.3.1 (UV-visible spectroscopy), can be calculated by the variation of the intensity of maximum absorbance (Eq. 2.27).

This information could be provided simpler from the spectral or concentration profiles got from MCR-ALS analysis. In addition the use of this tecnique is very useful in the case of overlapping, since it allows to obtain selective information. In this study the concentration profile was been exploited, so that Eq. 2.27 can be written as:

$$efficiency(\%) = \frac{C_0 - C_t}{C_0} \times 100 \qquad (3.1)$$

where C_0 is the initial concentration of dye A.R.97 and C_t the concentration of dye at time t.

Then, decolorization efficiencies, related to the four experiments, were compared in order to evaluate if and how the H_2O_2 concentration influences degradation.

- 4 -

RESULTS AND DISCUSSION

4.1 HANDLING DATA WITH MCR-ALS

In this section the most significant results, provided by chemometric treatment, are exposed. Particular attention is given to the first and third experiment. They can be considered as good patterns for explaining the whole results, since they represent two extreme situations: in Exp1 the process is carried out without oxidant, while in Exp3 a high concentration of H_2O_2 has been used.

4.1.2   UV-visible spectra

Fig.4.1 shows the UV-visible spectra obtained by the photooxidative process of dye A.R.97 during Exp1, while fig.4.2 shows UV-visible spectra of the photooxidative decolorization of dye A.R.97 (a) recorded during Exp3 and of the blank (b) recorded with the same experimental conditions of Exp3.

During the degradation of dye A.R.97, three wavelengths are relevant: a maximum of absorption at 495 nm and the bands at 308 and 236 nm. The band at 495 nm (attributed to $\eta\rightarrow\pi^*$ transitions of N=N, C=N and C=O chromophore groups) is responsible for the color of the dye solution. Absorbance bands at 308 and 236 nm ($\pi\rightarrow\pi^*$ transition in aromatic rings) represent the aromatic character of the dye [54].
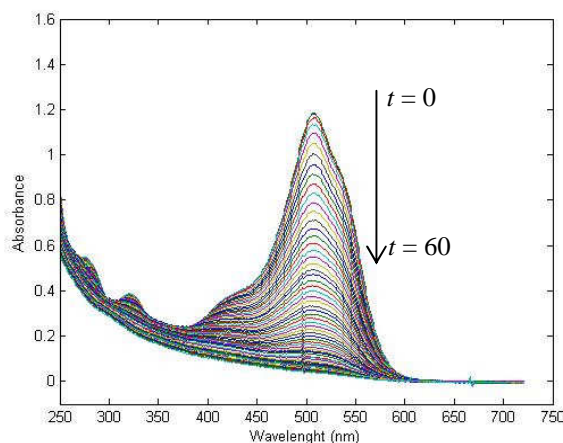

**Fig. 4.1 UV-visible spectra of the photooxidative
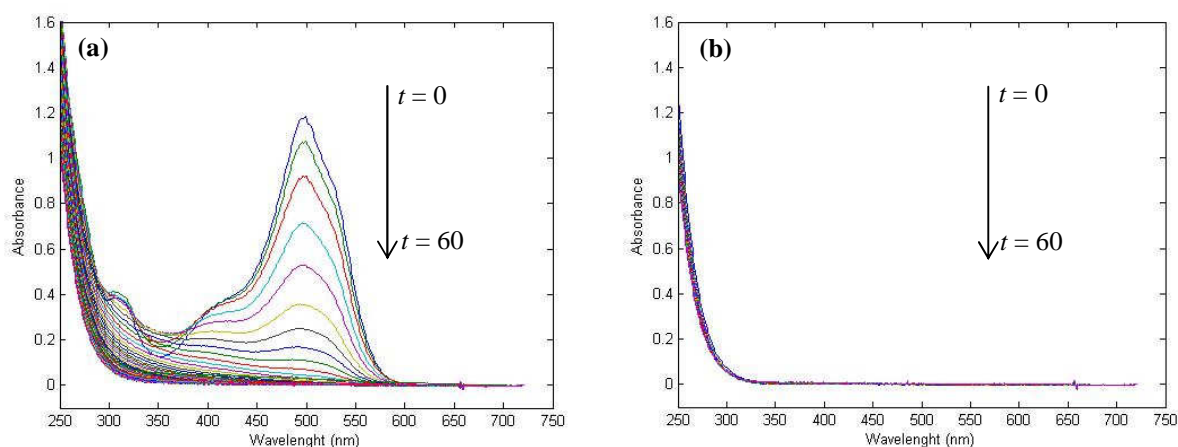decolorization of dye A.R.97 recorded during Exp1.**

**Fig. 4.2 UV-visible spectra of the photooxidative decolorization of dye A.R.97 (a) and the blank (b)
recorded during Exp3.**

The decrease in absorbance along time of peak with λ_{max} at 495 nm is due to the attack of the chromophoric part of the molecule and hence to the destruction of the extensive conjugated electronic system. Meantime the decrease in absorbance of peaks with λ_{max} at 308 and 236 nm corresponds to loss of aromaticity of the dye during the photodegradation. Such behaviour indicates, therefore, that dye degradation is on-going.

If figures 4.1 and 4.2a are compared, some differences can be noticed. In the first spectra are closer and thicker along the whole degradation time; instead, in fig. 4.2a spectra are initially more separated, above all for spectra related to the first minutes of the process. These differences can attributed to the fact that Exp1 was carried out without oxidant, while for Exp3 a concentration of H_2O_2 0.05 M has been used. It follows that the first degradation process is much more slower than the second, with minimal change in chemical composition, and therefore in absorbance, between consecutive spectra. Instead in Exp3 dye degrades faster and in particular the majority of chemical variation is concentrated in the first minutes of the process, with a more emphasized difference of absorbance.

In addition in fig. 4.2a the decrease in absorbance along the time is more stressed, appearing like a flattening. This trend is not present in fig. 4.1 and therefore it could infer that the complete degradation of dye was not achieved.

Spectra showed in fig. 4.2b are characterized by an absorbance below 300 nm, since in this case in the solution there is only H_2O_2, that not absorb in the visible region.

4.1.3   Data matrices

For each experiment the whole UV-visible spectra collected during degradation process has been arranged in two data matrix, named **E** and **B**, related to the degradation of dye and the degradation of H_2O_2 (assumed as blank) respectively. In fig. 4.3 the construction of matrix **E1** is proposed as an example.

Each matrix **E** (61 x 471) is characterized by 61 rows, that are the number of spectra collected for every minute (from 0 to 60 min), and 471 columns, that correspond to the absorbance (*A*) in the range measured (250-720 nm).

Matrix **B** (61 x 471), having the same dimensionality of matrix **E**, was created by the treatment of the data recorded during the degradation process of H_2O_2 only in the case of Exp2, 3 and 4, since in Exp1 the oxidant was not used.

The table 4.1 resumes the matrices produced in this first data handling for the four degradations carried out.

Tab. 4.1 Matrices produced by treatment of the data collected during the degradation of the dye and H_2O_2.

EXPERIMENT	MATRICES	
	DYE DEGRADATION	H_2O_2 DEGRADATION
Exp1	**E1** (61 x 471)	--
Exp2	**E2** (61 x 471)	**B2** (61 x 471)
Exp3	**E3** (61 x 471)	**B3** (61 x 471)
Exp4	**E4** (61 x 471)	**B4** (61 x 471)
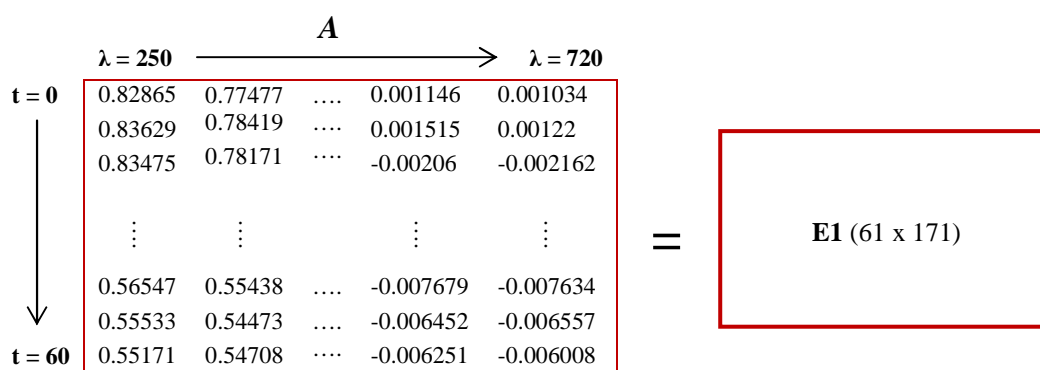
Fig. 4.3 Example for the construction of a degradation matrix. In this case E1.

4.1.4 Singular Value Decomposition

The two set of matrices, **E** and **B**, were analysed with SVD algorithm. The application of SVD enables to obtain for each matrix the singular values, describing the variance explained by an increasing number of components or factors.

Several methods can be used in order to decide the number of the significant components. Among these two different methods have been applied in this study, depending whether or not the oxidant, H_2O_2, was used.

In the case of Exp1 it was applied an approach based on the analysis of the *scree plot*. This is obtained plotting the explained variance for each singular value against the number of components. The analysis is lead observing the line trend in the plot: when there are significant components, the slope of the line will be steep, while, conversely, the slope will be flat. In plain word we consider significant the number of components, observable above a typical *elbow*, that explain the majority of the variance.

Fig. 4.4 shows the *scree plot* for the first seven singular values of matrix **E1**, collected in descending order in table 4.2. It is possible notice that after the third singular value there is a flattening of the line. Therefore, in this case, three singular values retain most of the explained variance.

Tab. 4.2 Singular values of E1.
Only the first seven values are shown.

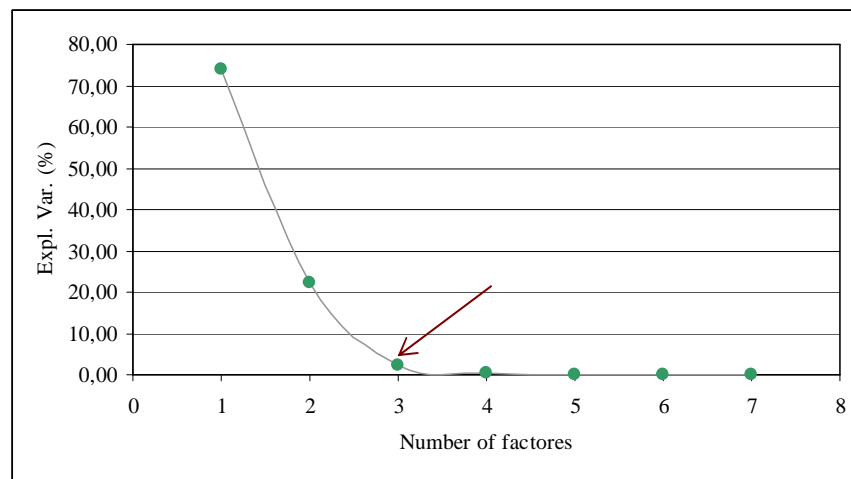| FACTORS	SINGULAR VALUES	EXPL. VAR. (%)
1	47,694	74,139
2	14,350	22,307
3	1,4728	2,289
4	0,18166	0,282
5	0,10438	0,162
6	0,04034	0,063
7	0,02969	0,046

Fig.4.4 Scree plot of the variance associated with the first singular values of D1.

Instead, since in the case of Exp2, 3 and 4, the degradation of H_2O_2 is assumed as the blank, it is possible to use the SVD results of matrix **B**. The first singular value obtained for **B** is related to H_2O_2 and this means that the second one is considered representative of the noise. Then, the comparison between this value and the singular values obtained from SVD analysis of **E** matrix, allows to determine how many components are meaningful: the singular values, that are greater than the noise value, are significant.

By way of example the case of Exp3 is discussed. Table 4.3 displays the singular values of **E3** and **B3** matrices. It emerges that four singular values might be significant in **E3** matrix, as they are greater than the second singular value of the blank, 0.29468, representative of the background level.

Tab. 4.3 Singular values of E3 and B3 matrices.
Only the first seven values are shown.

FACTORS	SINGULAR VALUES	
	B3	E3
1	25,305	36,808
2	0,29468	14,892
3	0,057363	3,6874
4	0,017294	0,80042
5	0,013801	0,16906
6	0,012375	0,093923
7	0,0117424	0,050574

4.1.5   Evolving Factor Analysis

Fig. 4.5 shows the EFA plot obtained analysing degradation matrix **E1**.

In the forward analysis, from the first minutes of degradation, the variability is explained by one factor (*f1*). Then at 9 min of reaction time, a new factor becomes relevant (*f2*), and a last one appears at 55 min (*f3*). According to Amrheim [55] the chemical rank of a spectra data matrix obtained analysing chemical reactions, is equal to the number of chemical species in the medium or equal to the number of independent reactions more one. Therefore in this case until 9 minute the chemical variability is

explained by one factor associated with the majority of untreated dye A.R.97, since until this time the dye degradation it is not significant. Then two factors are necessary to explain the chemical variability in the medium, which is characterized by the presence of at least a new chemical species. At the end the presence of another chemical situation is suggested as consequence of another reaction.

In the backward analysis, from 60 min to 41 min, there is only one factor (*b1*). From 41 to 5 min, the variability is explained by two factors (*b1/ b2*) and, at the end, a third one is observed after 5 min of degradation (*b3*).
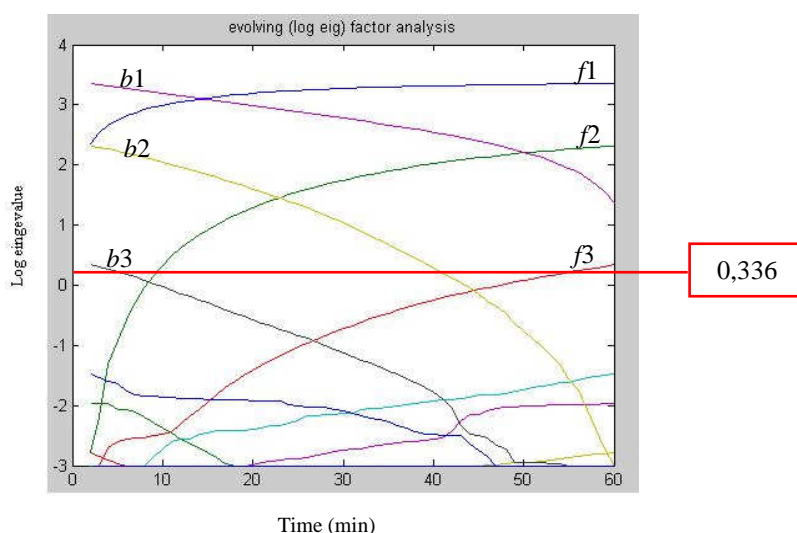
Fig. 4.5 EFA of the spectral data matrix E1. The red line represents the noise level.
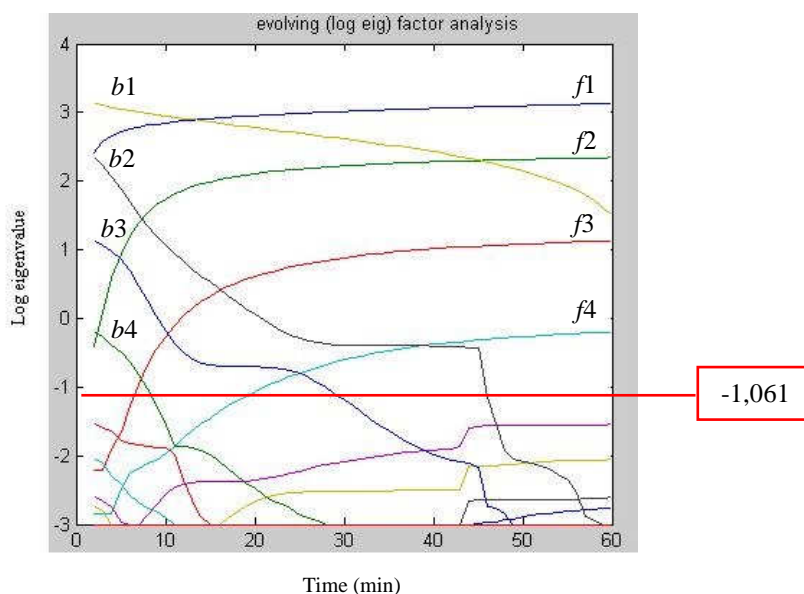
Fig. 4.6 EFA of the spectral data matrix E3. The red line represents the noise level.

Fig. 4.6 shows the EFA plot obtained analysing degradation matrix **E3**.

In the forward analysis from the first minutes of degradation, the variability is explained by two factors (*f1/ f2*); this indicates that from the beginning dye degradation is significant and hence new chemical species can be presented in the medium. At 5-7 min of reaction time, a new factor becomes relevant (*f3*), bringing new variability. This last is associated with the presence of new chemical species in the medium, involved in a new chemical reaction. A last factor appears at 20 min (*f4*); about it the same consideration could be done. Then, no additional information is obtained.

In the backward analysis, from 60 min to 45 min, there is only one factor (*b1*). From 45 to 30 min, the variability is explained by two factors (*b1/ b2*), then a third one is observed after 30 min of degradation (*b3*) and a fourth significant factor appears in the first minutes of the process at 10 min approximately (*b4*).

Therefore it could suppose that for **E1** at least three chemical species, active in the UV-visible region, could be involved in the process. On the other hand SVD and EFA analysis of **E3** indicate that probably four chemical species characterized the degradation. This difference could be explained considering that in presence of oxidant, i.e. in the case of Exp3, the degradation process is more complex. Therefore it is possible suppose that both the number of chemical reactions involved and the number of chemical species are higher respect to Exp1.

4.1.6   MCR-ALS analysis

Information about these species can be obtained by MCR-ALS analysis of **E1** and **E3** matrices. The process starts using the concentration profiles calculated by EFA as initial estimations.

*4.1.6.1 Analysis of **E1** concentration and spectral profiles*

Figure 4.7 depicts optimal concentration (a) and spectral (b) profiles which show the behaviour of the chemical species involved in the degradation process carried out

during Exp1. Table 4.4 shows the parameters used to evaluate the goodness of the optimization process for matrix **E1**.
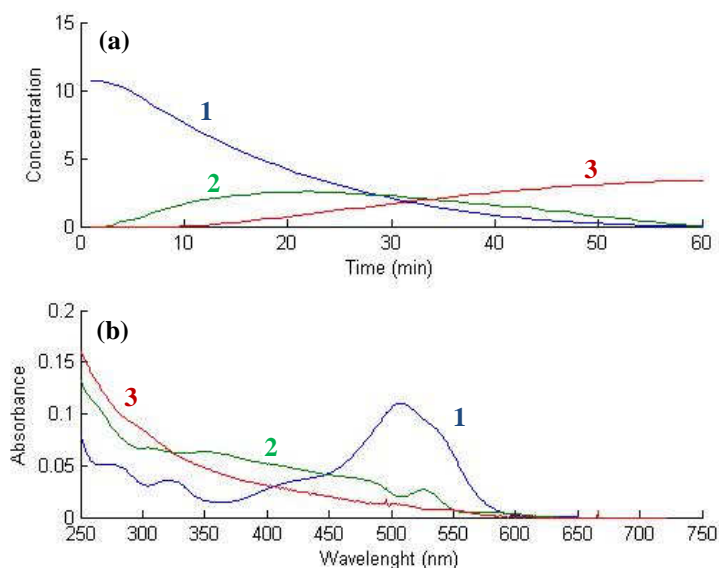

Fig. 4.7 Concentration (a) and spectral (b) profiles of the chemical species involved in the degradation processes retrieved by MCR-ALS for E1.

Tab. 4.4 Parameters used to evaluate the goodness of optimization process on E1.

LOF % PCA	R^2	r
0.535	99.9951	0.9687

It can observe that the spectral profiles (fig.4.7b) are characterized by the initial dye (1) that absorbs in the visible region and other species (2-3) which absorb at lower wavelengths. These profiles suggest that the azo dye degrades to form intermediates corresponding to smaller molecules that have high absorbance in the UV region.

It can noticed that species 2 present a maximum of absorbance around 350 nm, indicating the probable formation of intermediates containing aromatic systems and azo group. In fact an absorption at these wavelengths is characteristic of molecules like nitrobenzene. In addition this profile is also characterized by a peak of absorbance at wavelengths higher than the untreated dye.

The shape of the third spectrum (3), characterized by absorbance in UV region, indicates probably the formation of aromatic molecules product of the breakdown of azo linkage.

The concentration profiles (fig.4.7a) suggest that the initial dye (1) decreases along time, and it is near to zero after 50 min. Two other species are formed during the first minutes: one decreasing (2) and another one increasing (3) along the process. This behaviour suggests that species 2 and 3 could be refer to degradation intermediates and products respectively.

These results are in agreement with the EFA plot of matrix **E1** (fig.4.5). This is supported even by the parameters of goodness (tab. 4.4), which present good values.

*4.1.6.2 Analysis of **E3** concentration and spectral profiles*

Figures 4.8 depicts optimal concentration (a) and spectral (b) profiles which show the behaviour of the chemical species involved in the degradation process carried out in Exp3. Table 4.5 shows the parameters used to evaluate the goodness of the optimization process for matrix **E3**.
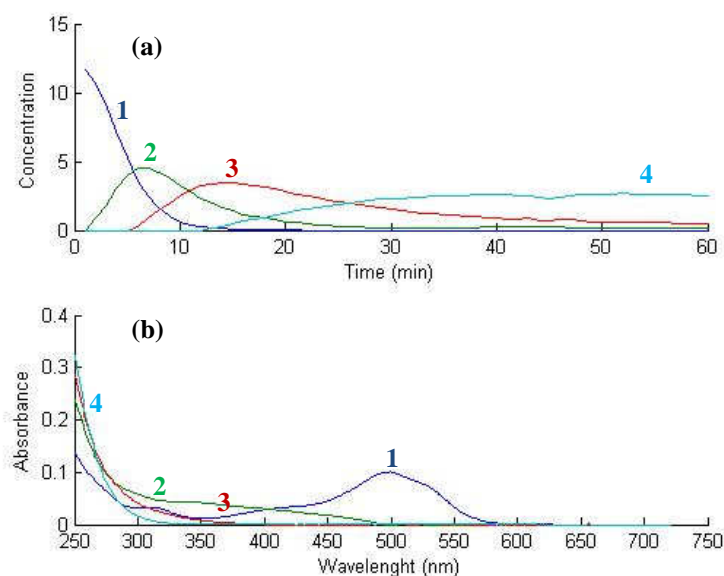

Fig. 4.8 Concentration (a) and spectral (b) profiles of the chemical species involved in the degradation processes retrieved by MCR-ALS for E3.

Tab. 4.5 Parameters used to evaluate the goodness of optimization process on E3.

LOF % PCA	R^2	r
6.0546	99.5987	0.9278

In the spectral profiles (fig. 4.8b) it can observe the profile of initial dye (1) and profiles of several species which present a high absorbance in the UV region, indicating that intermediate produced during the process are probable aromatic.

Among these only chemicals 3 present a more evident absorb between 300 and 400 nm. It is probable that this chemicals correspond to aromatic molecules with azo group.

In the concentration profiles (fig. 4.8a) at the beginning of degradation the initial dye (1) and other chemical species (2) are present. Dye decreases along time and in particular it is near to zero at the 15 min. Species 2, after an initial increasing, start decreasing then 5 min. There are also two more species: ones (3) appear at 7 min and then decrease, and another ones (4) that appear at 10 min and then increase. Therefore chemicals 2 and 3 could be considered as two different degradation intermediates formed at different times and chemicals 4 as degradation products.

This behaviour is in agreement with EFA plot of matrix **E3** (fig.4.8) and is confirmed even by the parameters of optimization goodness (tab. 4.5) which show good values.

4.2   MASS SPECTROMETRY ANALYSIS

4.2.1   Samples collecting

In light of what said up to this point the degradation process carried out without oxidant during Exp1 is the slowest one. It follows that this experiment is also the most suitable for determining more clearly the evolution of intermediate species during the process. For this reason it has been chosen for collecting several samples to perform a MS analysis in order to determine the hypothetic intermediate produced and hence to propose a general degradation pathway.

In order to analyze samples representative of the different chemical situations occurred along the process, the information shown in EFA plot (fig.4.5) has been taking into account. Consequently six samples were collected at 0, 3, 20, 35, 50 and 60 min:

- t = 0 and t = 3 are relative to the beginning and the first minutes of the process respectively;
- at t = 20 a second component appears, so that two chemical species are at least present;
- at t = 35 the process is at half of this path;
- at t = 50 a new component is appearing and three chemical species are at least present;
- the previous situation is emphasized at t = 60, namely at the end of the process.

4.2.2   Analysis of MS spectra: determination of degradation intermediates

The analysis of samples collected has provided six MS spectra. The interpretation of them has been comples cause the instrumental noise and the presence of a huge number of molecules produced during the degradation. However it has tried to determine the most significant chemical species.

Fig. 4.11 shows the spectrum related to the sample collected at the beginning of reaction (t=0), meaning the spectrum of the initial untreated dye A.R.97 ($C_{32}H_{20}N_4Na_2O_8S_2$; MW = 698.61). Three majority peaks are observed:

a) at 675.62 m/z corresponding to the dye without one Na^+: $[C_{32}H_{20}N_4NaO_8S_2]^-$;

b) at 653.70 m/z corresponding to the dye without two Na^+, of which one is substituted by H^+: $[C_{32}H_{21}N_4O_8S_2]^-$;

c) at 326.32 m/z resulting from the loss of two Na^+ and hence corresponding to the molecule dye with two charges: $[C_{16}H_{10}N_2O_4S]^{2-}$.

Molecular species associated with these characteristic peaks of dye A.R.97 are detailed in table 4.7. At t=3 min (spectrum not shown) the abundance of these three peaks starts to decreases and no other changes are noticed.
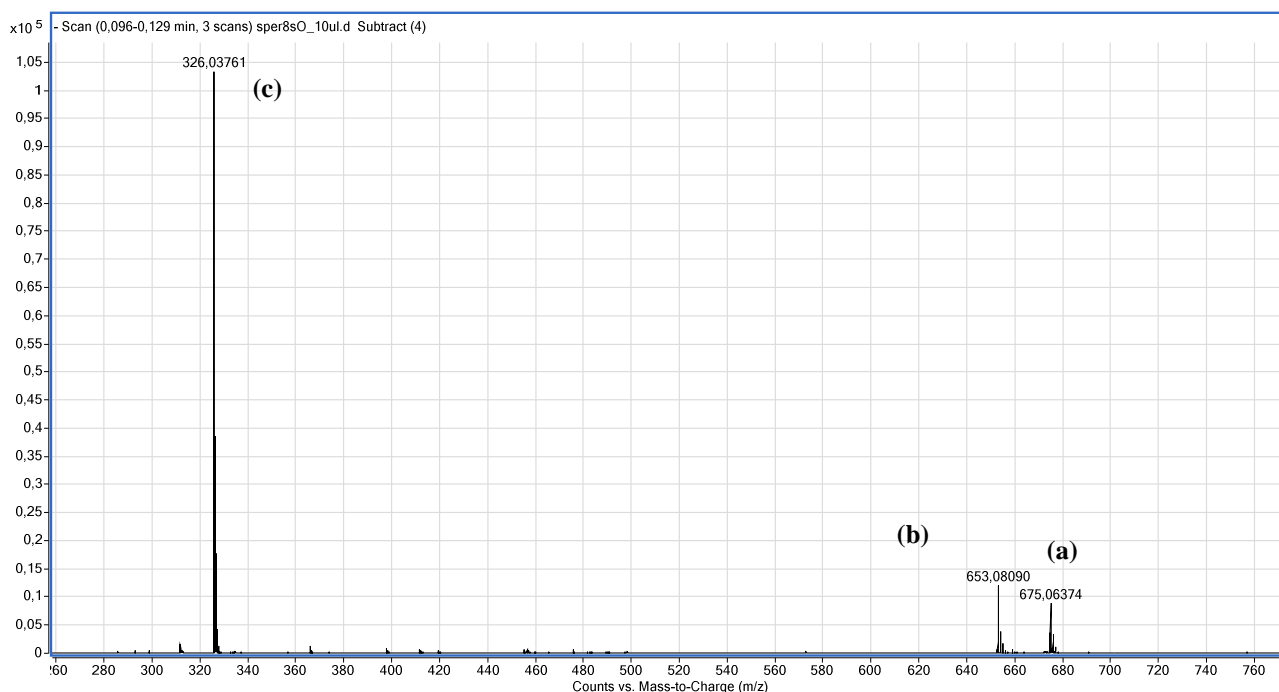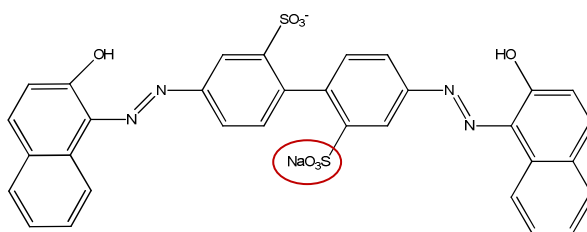

Fig. 4.11 MS spectrum of the dye A.R.97 degradation process at time t=0 min.
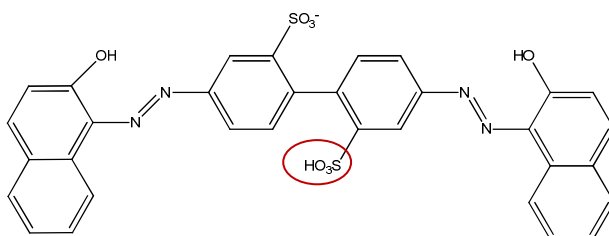
Tab. 4.7 Characteristic peaks of dye A.R.97.

(a)

675.62 m/z

(b)

653.70 m/z

(c)

326.32 m/z

Four new peaks appear at t=20 min (fig.4.12). The molecular species associated to these peaks are presented in table 4.8. Two of them could be referred to first oxidation forms: $[C_{32}H_{22}N_4O_9S_2]^{2-}$ at 343.04 m/z and $[C_{32}H_{21}N_4O_9S_2]^{2-}$ at 334.03 m/z. The peak at 257.01 m/z, corresponding to $[C_{22}H_{16}N_3O_8S_2]^-$, could be resulted from the breaking of an azo linkage. There is another peak at 351.04 m/z probably due to a dimerization reaction.

Fig.4.13 shows the most informative part of the spectrum related to t=35 min. The spectrum details a more complex situation than before: peaks associated with the initial dye decrease in size and in the meantime an elevated number of new peaks appears. Three groups of peaks, indicated in fig. 4.13 within different color circles, can be distinguished:

I- peaks at high molecular weights referred to first oxidation molecular species;

II- peaks at intermediate molecular weights associated with molecular species produced by the breaking of azo linkages;

III- peaks at low molecular weights related to molecular species resulted from the opening and oxidation of aromatic rings.

Table 4.8 reports the possible molecular species related to some peaks of the three groups.

Peaks of group I (yellow circle), already appeared at 20 min, start to decrease in size.

Simultaneously news peaks appear. Part of these, belonging to group II (green circle), can be considered a huge cluster of reaction intermediates difficult to detect. This might be due to their transient nature, so that these compounds are rapidly transformed in other species. For the group II some determined peaks are: the peak at 257.01 m/z, already presented at 20 min, and corresponding to $[C_{22}H_{16}N_3O_8S_2]^-$, the peak at 265.01 m/z related to $[C_{12}H_8O_5S]^-$ and the peak at 197.21 m/z corresponding to $[C_{12}H_9N_2O]^-$.

At this time other peaks, included in group III (red circle), emerge. Among these some relevant peaks are: at 181.01 m/z corresponding to $[C_8H_5O_5]^-$, 165.02 m/z related to $[C_8H_5O_4]^-$, 149.02 m/z related to $[C_8H_3O_3]^-$, 137.02 m/z related to $[C_7H_6O_2N]^-$, 121.03 m/z corresponding to $[C_7H_5O_2]^-$, and 105.02 m/z corresponding to $[C_7H_5O]^-$.
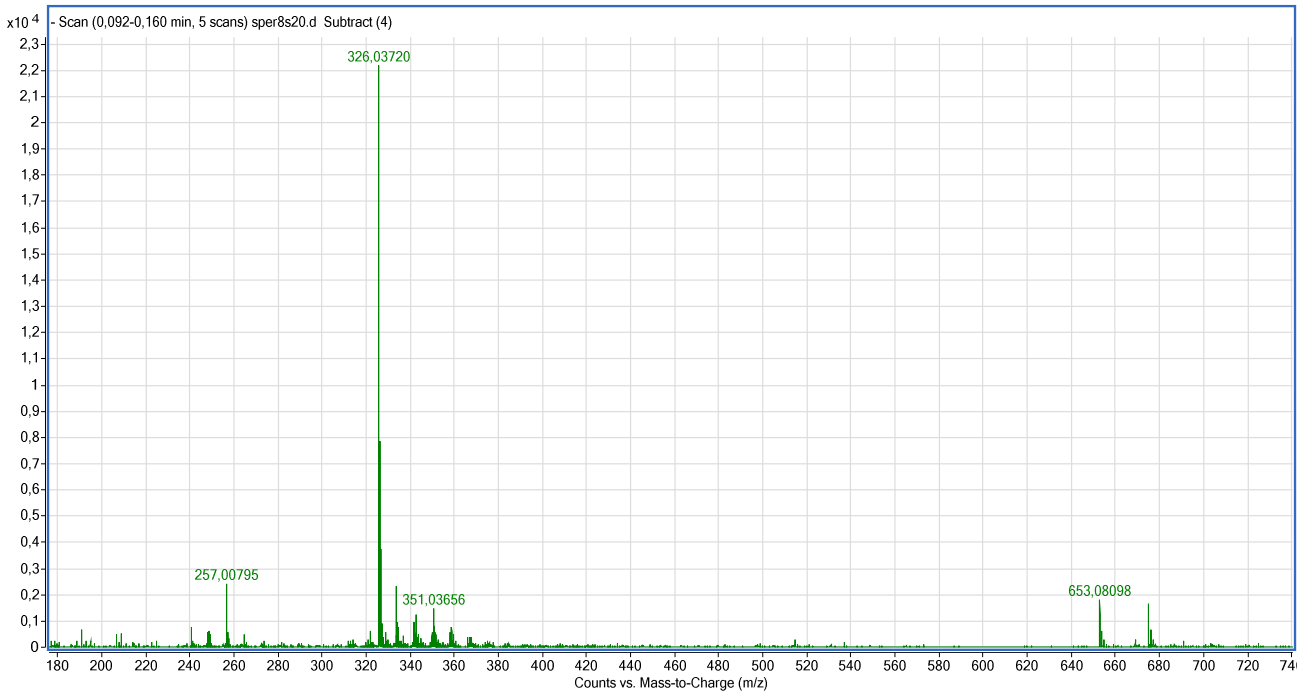
Fig. 4.12 MS spectrum of dye A.R.97 degradation process at time t=20 min.
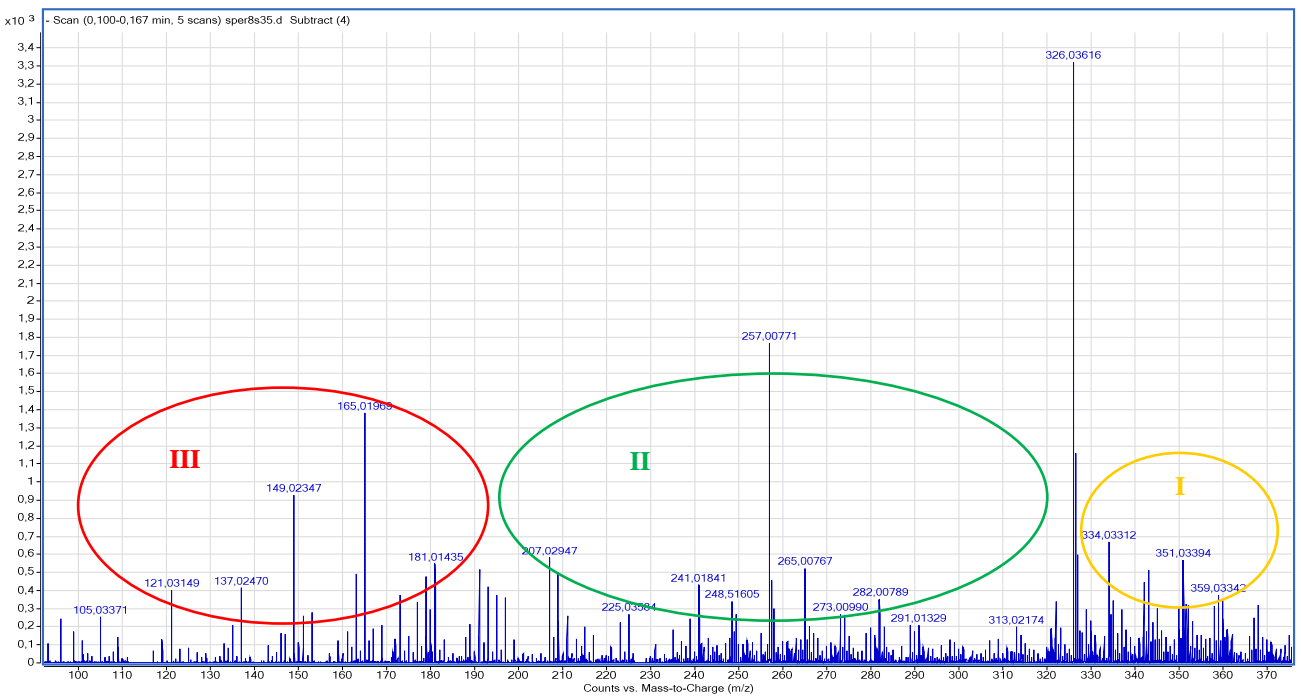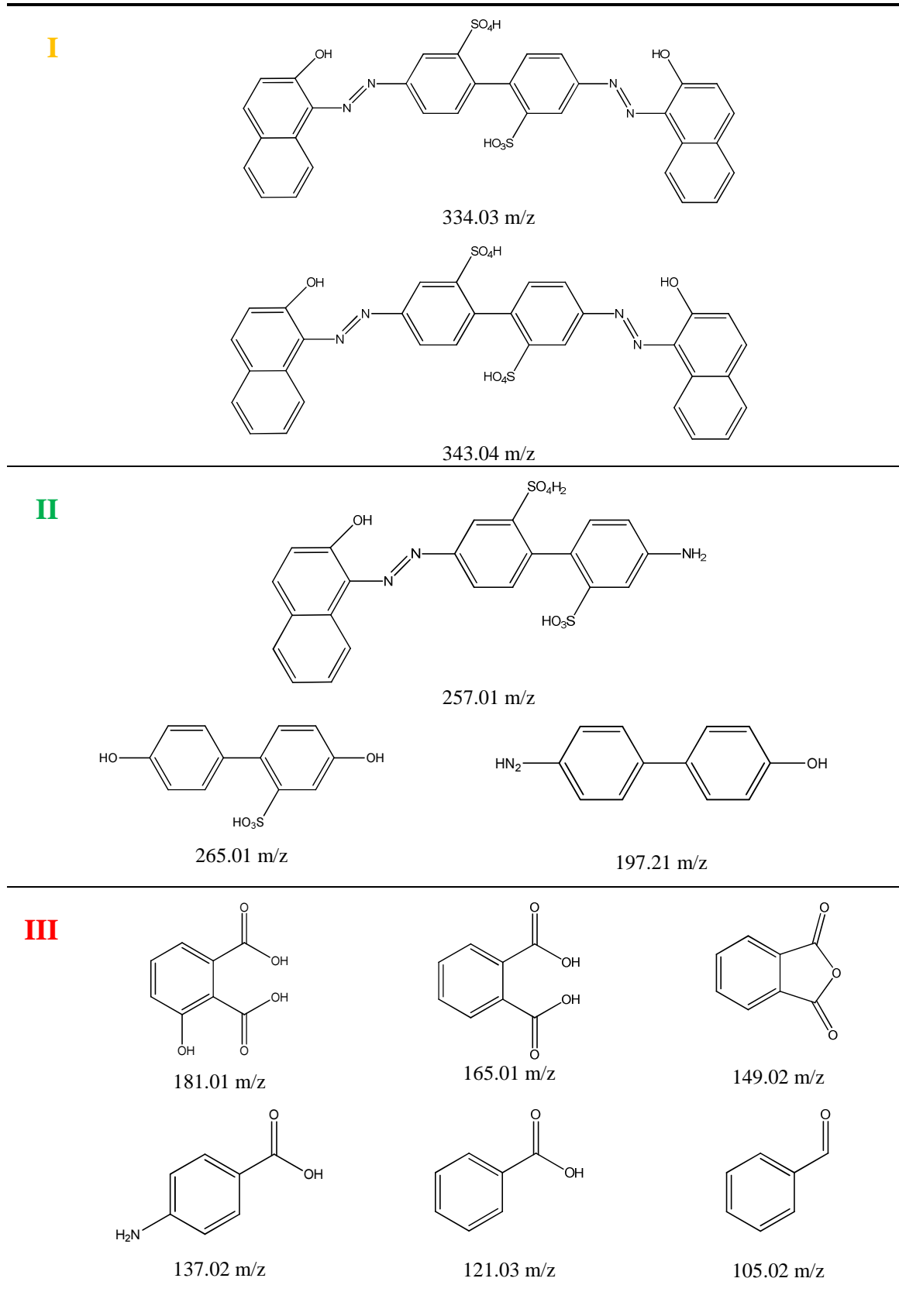

Fig. 4.13 MS spectrum of dye A.R.97 degradation process at time t=35 min.

Tab. 4.8 Hypothetic molecular species related to the peaks of the spectrum of time t=35.

I

334.03 m/z

343.04 m/z

II

257.01 m/z

265.01 m/z

197.21 m/z

III

181.01 m/z

165.01 m/z

149.02 m/z

137.02 m/z

121.03 m/z

105.02 m/z

At 50 min (fig. 4.15) peaks related to the untreated dye, to the oxidative forms and peaks of the second groups decrease drastically in size, while peaks of group III increase. At these time new peaks start to appear at lower m/z: at 95.95 m/z corresponding to $[HSO_4]^-$, 89.02 m/z corresponding to $[C_2HO_4]^-$ and 72.99 m/z corresponding to $[C_4HO_3]^-$. The hypothetic molecular species determined from these peaks are represented in fig. 4.14.

This situation becomes more evident at time t=60 (fig. 4.16) corresponding to the end of the degradation process. Compared to previous time, t=50, there are not new peaks. Several important information can be obtained from this last spectrum:

- peaks associated with the initial dye are now disappeared;
- peaks at higher molecular weight (yellow circle in fig. 4.13) are disappeared;
- peaks at intermediate molecular weights (green circle) are decreasing in size;
- peaks at lower molecular weights (red circle) are significantly increasing in size.

If the two figures 4.13 and 4.16 are compared, it is possible to see more clearly the changes occurred during the degradation process, taking into account the differences between the areas of the circles.
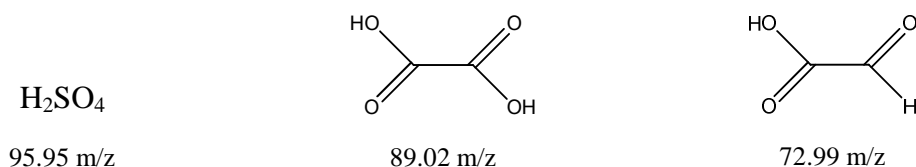
H_2SO_4

95.95 m/z

89.02 m/z

72.99 m/z

Fig. 4.14 Hypothetic molecular species related to new peaks appears at time t=50.
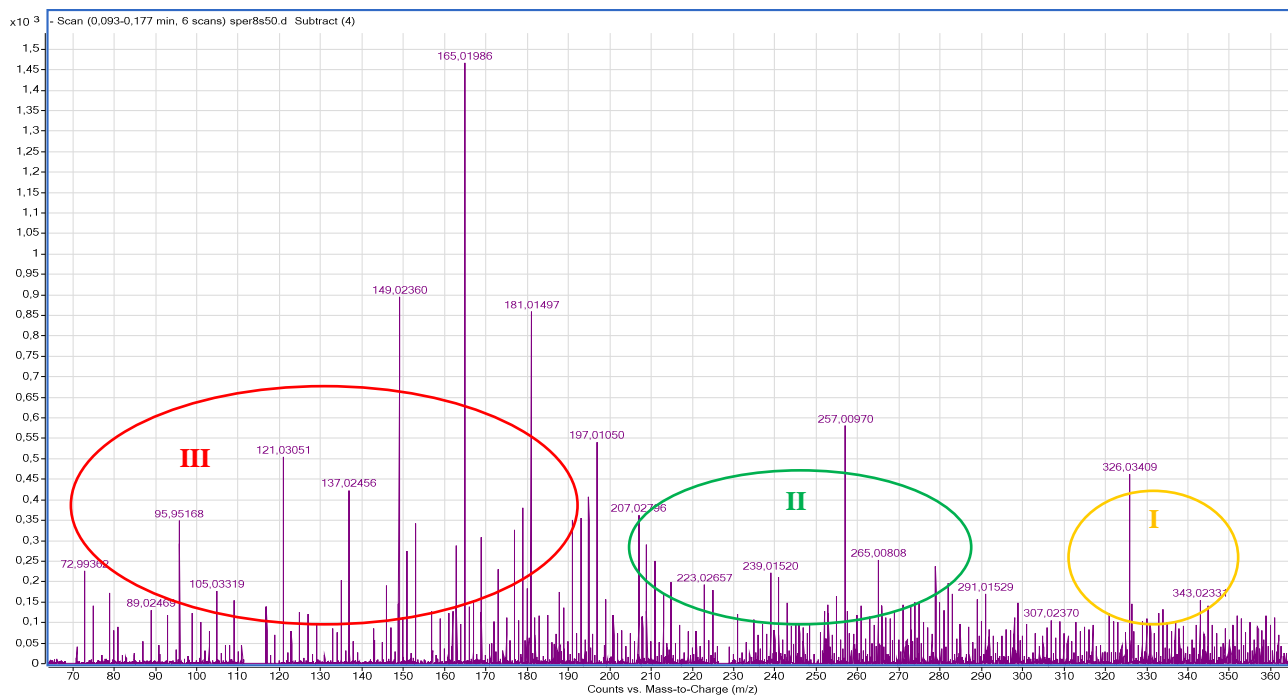
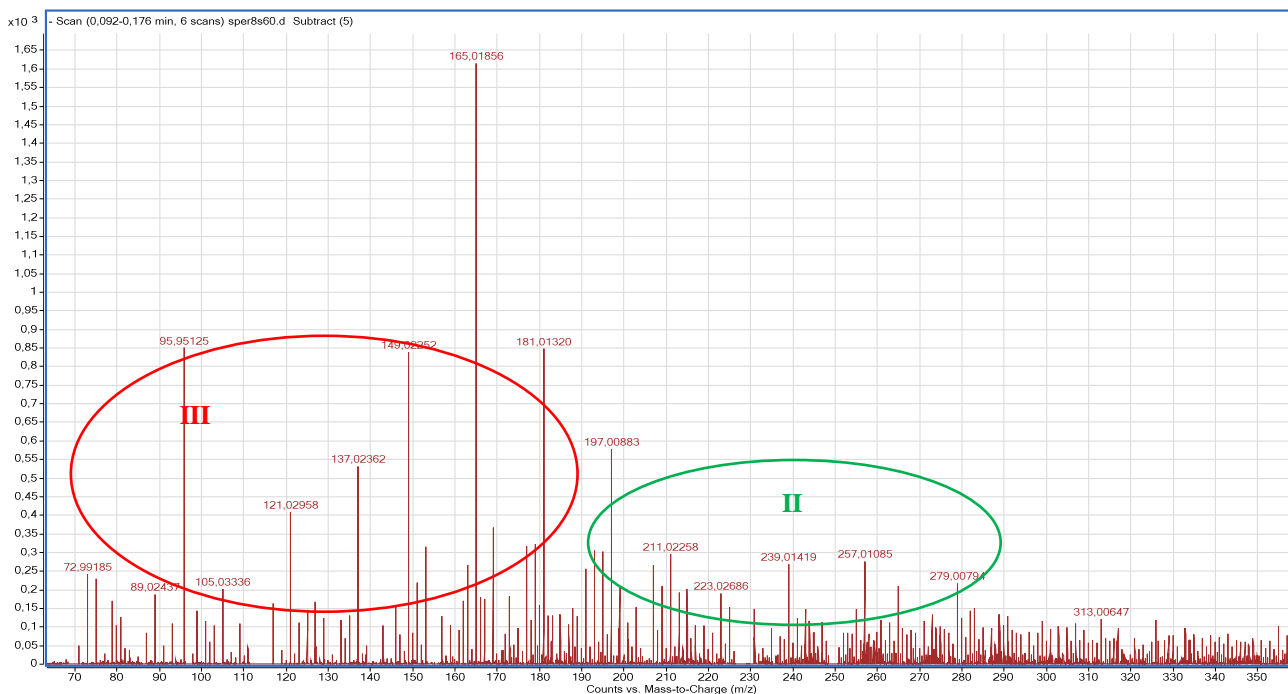**Fig. 4.15 MS spectrum of dye A.R.97 degradation process at time t=50 min.**

Fig. 4.16 MS spectrum of dye A.R.97 degradation process at time t=60 min.

4.2.3 Determination of a reaction pathway

Due to the complex molecular structure of dye A.R.97 the identification of many intermediates was rather complicated. Despite of this, taking into account the analysis of MS spectra, a reaction pathway for the degradation of the dye studied has been postuleted. The proposed reaction scheme is detailed in fig. 4.17.

The first step (a) involves the oxidation of dye A.R.97, followed by azo bonds breaking (b). This causes the destruction of the chromophore (-N=N-) and consequently the loss of the aromatic conjugation. This reaction could be favourite also by the azo-hydrazone tautomerism characterizing dye A.R.97.

In the third step, after the hydroxylation of intermediates produced, hydroxylated derivates are oxidized to the quinoid structure (c). This is followed by the opening of aromatic rings and the production of carboxylic acids (d). At the end the opening rings undergo further oxidation processes, and the final degradation products could be CO_2 and H_2O. This last situation is achieved only when the degradation process reaches the *mineralization*; however this not seems to have occurred for the degradation process studied.

It is also more likely that ionic forms such as NO_3^- and SO_4^{2-} are released in the course of the degradation.

(a) Oxidation

I

(b) Azo bonds breaking

II

(c) Hydroxilation

III
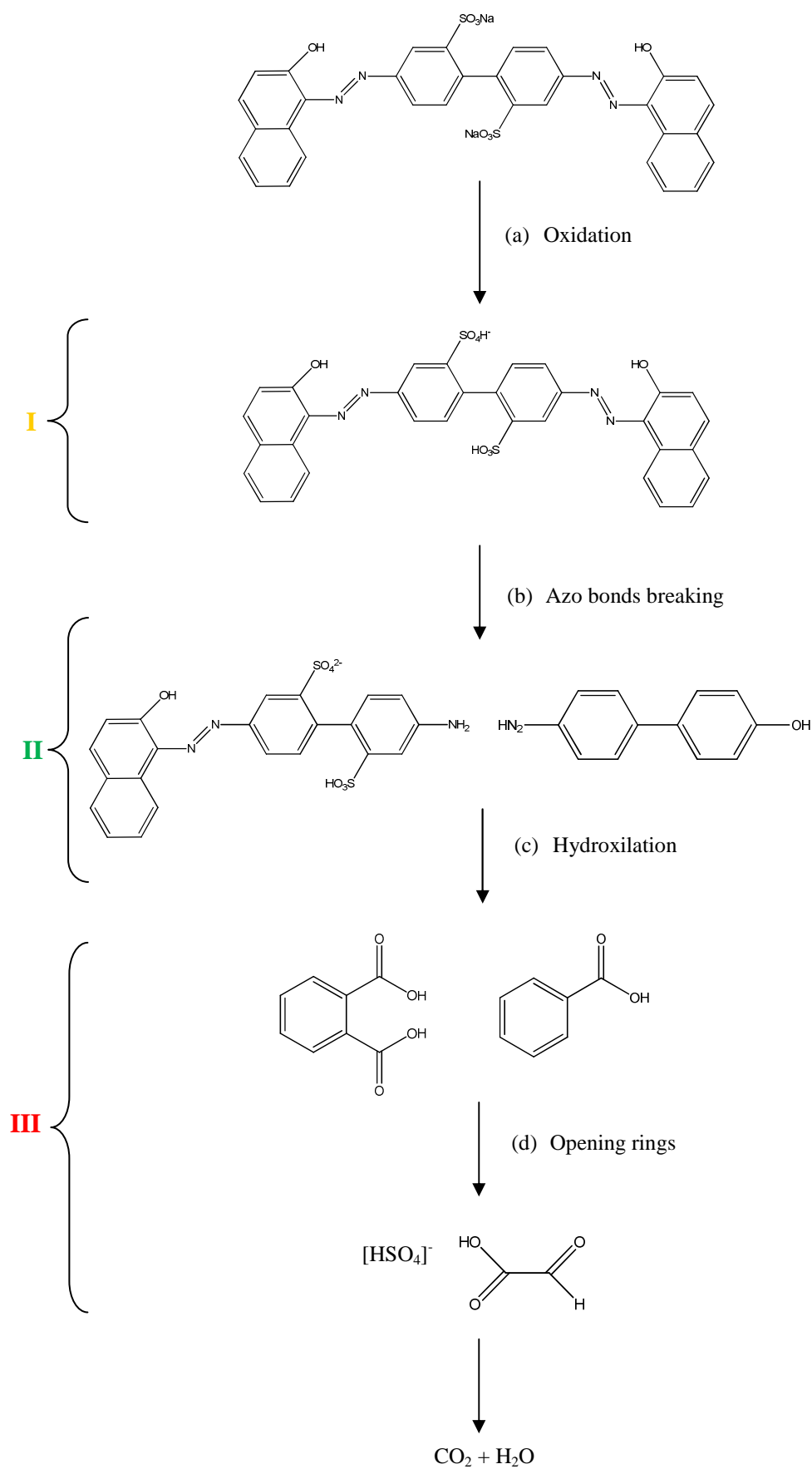
(d) Opening rings

$[HSO_4]^-$

$CO_2 + H_2O$

Fig. 4.17 Hypothetic reaction pathway proposed for dye A.R.97 photooxidative decolorization.

4.2.3.1 General discussion over chemometric results and Mass Spectrometry analysis

Chemometric results and mass spectrometer results can be considered as two complementary approximations for the study of the same process, the degradation of dye A.R.97. The chemometric approach gives a first probably overview of the studying system: how it could change in time, how much chemicals could be implied in the process and what is their behaviour. Consequently chemometrics provides also the information necessary to carry out the follow MS analysis, i.e. the times for the collection of the samples to be analysed.

On the other hand mass spectrometer analysis allows to define the molecular structure of these chemicals and what is likely the chemical reaction occurred during the process.

Therefore only discussing jointly these different but synergic results, it will be possible to understand more deeply the degradation process of the dye A.R.97.

For this purpose the concentration and spectral profiles retrieved with MCR-ALS for matrix **E1** are again proposed in the fig. 4.18.
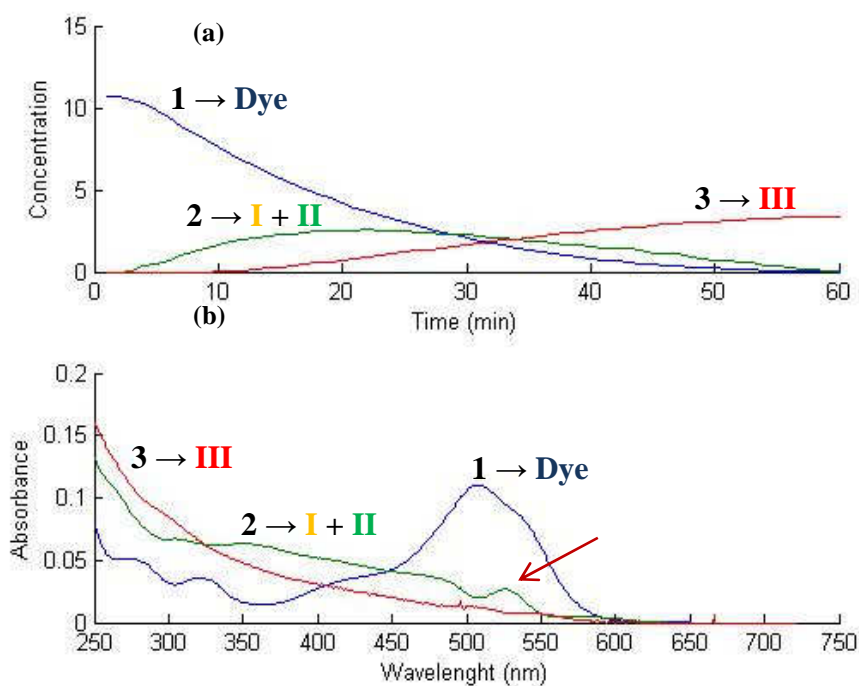

Fig. 4.18 Concentration (a) and spectral (b) profiles of the chemical species involved in the degradation processes retrieved by MCR-ALS for E1.

The proposed reaction pathway starts from the untreated dye A.R.97, corresponding to chemicals 1. In agreement with concentration profile also in the MS analysis it is observed that the initial dye decreases in size along the process.

The molecules, belonging to group II determined during MS analysis (fig.4.13), could be associated with chemical species 2. These molecules, formed from the azo bonds breaking, continue to be large aromatic systems and some of them contain at least one azo linkage, as indicating by the absorbance in the wavelengths region 350-400 nm. This kind of structure agrees with the spectral profile of chemical species 2.

In addition, as the concentration profile shows, chemical species 2 decrease in size after 30 min simultaneously to the increasing of chemical species 3. The same trend is evident in the spectrum at 35 min (fig.4.13), in which peaks of group II are decreasing and present abundances lower than peaks of group III that are increasing in size. It suggests that chemical species 2 could be considered degradation intermediates that are consumed during the reaction consequently to the formation of chemicals 3, the degradation products.

Chemical species 3 could correspond to aromatic compounds, included in group III (fig.4.13). These molecules absorb in the UV region and increase in size after 20 min of the process.

Group III includes also low molecular weight compounds which have been formed during the process, such as NO_3^- and SO_4^{2-}. These molecules are not active in the UV-visible region studied and therefore are not visible in the fig.4.18. In addition the final reaction products, CO_2 and H_2O, are other molecules undetectable in the studied wavelengths range and hence they are not observed at the end on the degradation.

The oxidative species, included in group I, seem to not have a correspondence. In fact the presence of oxidative forms should show an absorbance at wavelengths higher than that of untreated dye due to the increasing of resonance. This is observed over the profile of chemical species 2 as a low peak, as indicates by the red arrow in fig. 4.18b.

In addition, referring to MS analysis results, two different groups of aromatic molecules with azo groups have been detected at intermediate times of the process.

These groups include oxidative forms (I) and molecules obtained from the attack of azo linkage (II). It suggests that two intermediates are formed during the degradation.

Therefore there seems to be a contrast between chemometric results and MS analysis. Really this apparent non concordance could be explained considering that:

1- EFA analysis provides the number of chemical situations occurred during the process and that this number is not necessary equal to the number of chemical species formed;

2- chemical species included in group II is similar to chemical species of group I, so that they are not distinguished by UV-vis spectroscopy analysis and hence appear jointly in a unique profile (2) in the MCR-ALS analysis.

This apparent contrast is, therefore, due mainly to the low selectivity of the analytical technique used, i.e. UV-vis spectroscopy. This last cannot distinguish the two intermediates formed during the degradation cause to their similar molecular structures and their fleeting nature as they are rapidly transformed in other chemical species.

4.3 EVALUATION OF INFLUENCE OF H_2O_2 CONCENTRATION

The evaluation of influence of H_2O_2 concentration over the trend of degradation process can be done comparing the chemometric results and the decolorization efficiency (Dec. Eff.) for the four experiments.

Really Dec. Eff. and MCR-ALS results are closely related, as the last provides the concentration profiles used for the calculation of the first.

4.3.1 Results of optimization process of degradation matrices set

Table 4.9 reports the values of parameters used to evaluate the goodness of optimization process carried out for the four degradation matrices.

It can be noticed that matrix **E1** provides the best values. In addition the values get worse as more hydrogen peroxide is added, so that in a decreasing scale it results: **E1** > **E2** ≥ **E3** > **E4**.

In particular values of **E4**, the worst ones, are detached from values of other matrices, that can be considered in general good. This suggests that in the case of Exp4 the chemical system is too much complex to be analysed without overstraining the algorithm of optimization.

This situation is observed clearly also in fig. 4.19 and 4.20. The first shows the spectra of the degradation of dye A.R.97 (a) and the oxidant (b) collected during Exp4. It can noticed that during the first minutes the spectra of dye degradation are quite separated, indicating that degradation occurs rapidly due to the elevate amount of oxidant presented in the initial solution. This situation leads a lack of information relatively to the whole process, so that a good MCR-ALS analysis cannot carried out.

The presence of a system highly complex is also evident in EFA plot (fig. 4.20), in which it is possible notice even an elevated background noise.

For these reasons chemometric results obtained by handling data spectra of Exp4 must be considered not reliable enough, since UV-vis spectroscopy cannot detective sufficiently well dye and chemical species formed during degradation due to the rapidity of the process in the first minutes.

Tab. 4.9 Values of parameters of goodness for optimization process.

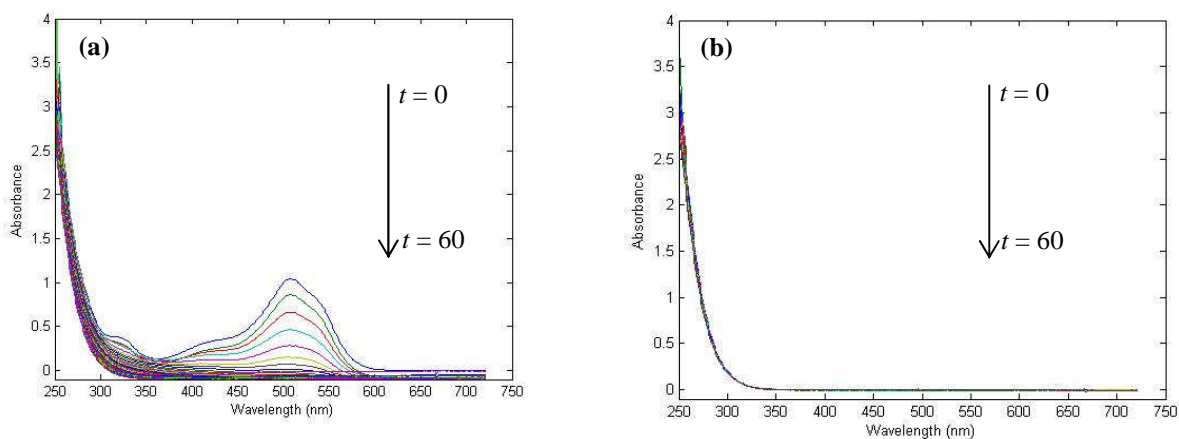| MATRICES	N. COMPON.	LOF % PCA	R^2	r
E1	3	0.535	99.9951	0.9687
E2	4	2.0362	99.9535	0.9266
E3	4	6.0546	99.5987	0.9278
E4	6	15.3003	97.644	0.6344

Fig. 4.19 UV-visible spectra of the photooxidative decolorization of dye A.R.97 (a) and the blank (b) recorded during Exp4.
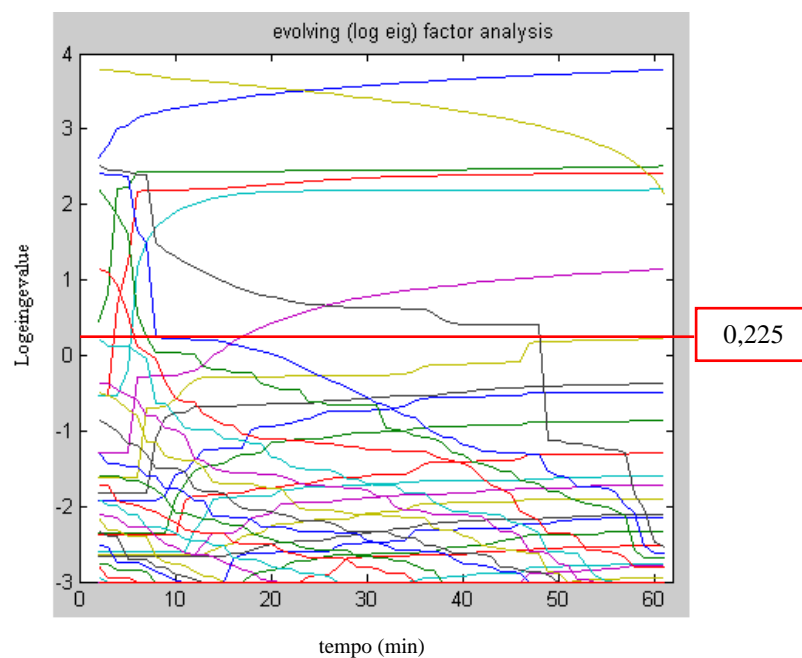

Fig. 4.20 EFA of the spectral data matrix E4. The red line represents the noise level.

4.3.2 Determination of decolorization efficiency

From chemometric analysis results that values obtained for Exp4 are not reliable. Therefore, the *decolorization efficiency (%)* (Dec. Eff.) was calculated only for the first three experiments (exp1-2-3) by the Eq. 3.1 using the concentration profiles retrieved by MCR-ALS.

Table 4.10 presents the Dec. Eff. for the three experiments, initially for every minute until the tenth and then for every five minutes.

Table 4.10 Variation of the decolorization efficiency (%) during the four degradations.

TIME (min)	Exp1 - NO H_2O_2	Exp2 - 0.02 M H_2O_2	Exp3 - 0.05 M H_2O_2
0	0	0,00	0
1	0	11,08	8,23
2	1,55	31,92	20,41
3	4,14	55,31	38,38
4	7,85	73,86	54,33
5	12,03	86,17	69,31
6	16,37	93,66	78,80
7	20,74	97,52	85,96
8	24,69	99,51	90,97
9	28,75	100	94,51
10	32,53	100	96,52
15	49,75	100	99,61
20	63,29	100	99,99
25	73,71	100	100
30	82,12	100	100
35	88,68	100	100
40	93,31	100	100
45	96,17	100	100
50	98,25	100	100
55	99,48	100	100
60	100	100	100

According to table 4.10 the complete degradation of dye A.R.97, corresponding to 100% of Dec. Eff., is reached in different times for the four processes:

- Exp1 → 60 min (at the end of the process);

- Exp2 → 9 min;
- Exp3 → 21 min;

It follows that the fastest degradation occurs in Exp2 and the slowest one in Exp1.

This situation is explained more clearly in fig. 4.19, in which variation of Dec. Eff. is plotted against time. The three processes show different trends. Exp1 shows a trend suggesting that a gradual degradation has occurred during all the process. On the other hand Exp2 and Exp3 present a similar shape: the rate of decolorization increases very steeply in the first ten minutes and then remain constant, meaning that dye is almost completely degraded into the first minutes of the process.

For Exp3 an inhibition of degradation process is observed. This could be due to the excess of H_2O_2, that acts with OH• radicals favouring the production of hydroperoxyl radicals, HO_2•, which are much less reactive and not contribute to the oxidative degradation of organic substrate. The consequent result is a reduction of the efficiency of dye degradation.
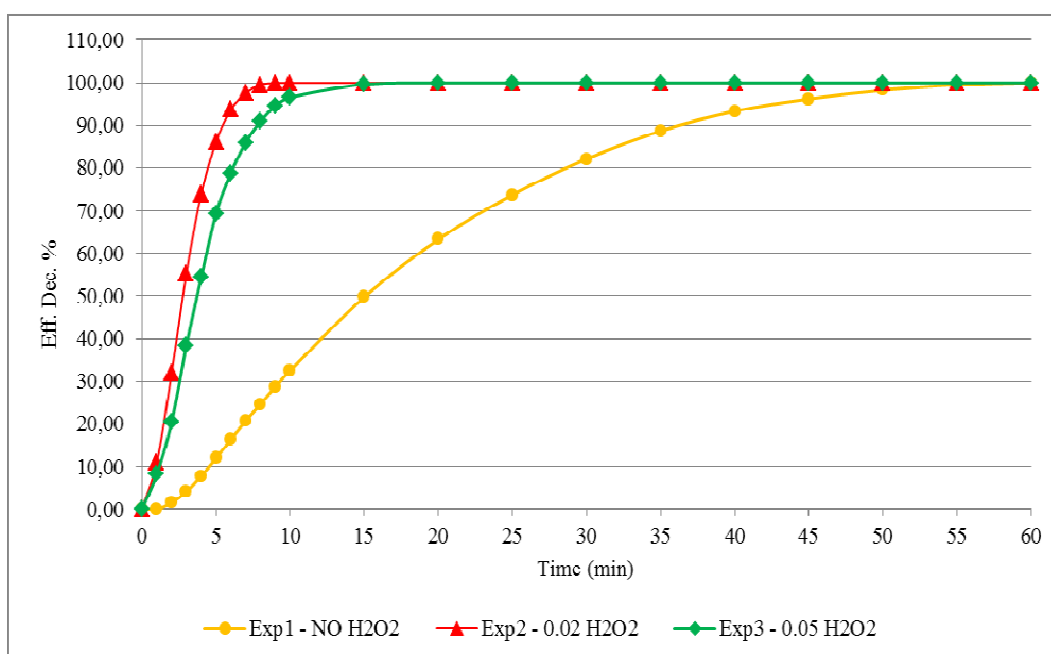

Fig. 4.19 Decolorization efficiency plotted against the time.

- 5 -

CONCLUSION

The aim of the study presented was to *develop an analytical methodology, based on a chemometric approach, able to investigate complex system without specific analytical signal*. This methodology was exploited for the analysis of the photodegradation process of the acid azo dye A.R.97 in presence of oxygen peroxide, H_2O_2, as oxidant.

The analysis has been carried out monitoring the photodegradation process through UV-visible spectroscopy and employing chemometric tools. These have been used for handling the chemical information contained in the UV-visible spectra recorded along the process.

Three principal analytical points connected to each other have been developed:

1. Chemometric treatment of the UV-visible data collected during the degradation process by means of multivariate tools, such as Singular Value Decomposition (SVD), Evolving Factor Analysis (EFA) and Multivariate Curve Resolution method with Alternative Least Square (MCR-ALS).

2. Mass Spectrometry (MS) analysis of some representative samples, taken during the degradation process, in order to identify the degradation intermediates and propose a reaction pathway.

3. Investigation of the role of the concentration of H_2O_2 on the degradation trend, as it is one of the most important influential factors in the H_2O_2/UV photolysis.

The chemometric analysis of the data collected during the experiments has given two fundamental results:

- during the degradation process several compounds are produced. These last show different behaviour: they appear and disappear at different times as extrapolated from EFA plot, they have different concentration rates as it is visible in concentration profiles and they present absorbance in different wavelength ranges as indicated in spectral profiles. In this way it was possible obtain a first framework of the chemical nature of these compounds;

- it has allowed to determine that the slower experiment is that carried out without H_2O_2 (Exp1), which permits to visualize better the evolution of the process and, in particular, the moments in which each intermediate is formed.

These results have been exploited for setting the MS analysis and for carrying out the analysis of the influence of H_2O_2 concentration.

The EFA plot has provided a valuable tool for the selection of six times of the process in which collecting six samples representative of the different chemical situations occurred along the degradation of Exp1.

The Mass Spectrometer analysis was implemented over these six samples and has allowed to define a possible reaction pathway for the degradation process, that could be described as follow:

- the process starts from untreated dye A.R.97;

- initially the dye is oxidative and high molecular weight compounds are detective;

- in a second step azo linkage are broken and intermediate molecular weight compounds are formed;

- at the end degradation products are formed. These corresponded to low molecular weight aromatic compounds.

It follows that during the process two different degradation intermediates are formed. Then they are consumed consequently to the formation of degradation products.

From the analysis of the *Decolorization Efficiency (%)* it results that the most rapid degradation occurs during Exp2, namely with an intermediate H_2O_2 concentration, that in this case was of 0.02 M. Without oxidant the degradation occurs very slowly as in Exp1, while at higher concentration of H_2O_2 the process is inhibited with a consequence slowdown of dye degradation as in Exp3, where a H_2O_2 0.05 M have been

used. The inhibition of the process is attributed to the excess of H_2O_2, which leads to production of hydroperoxyl radicals, $HO_2\bullet$, that not contribute to the oxidative degradation.

The employment of UV-visible spectroscopy has appeared to be the main limitation of the methodology due to its low selectivity. This was clear for Exp4, in which a H_2O_2 0.1 M has been used, and for the determination of degradation intermediates. In this last case the two chemical intermediates have not been distinguished cause the similar molecular structure, namely cause the similar absorbance. For Exp4 the fastness of degradation along the first minutes has not provided sufficient information to carried out a good chemometric analysis. However it must be remembered that UV-visible spectroscopy is a simple, fast and not expensive analytical technique, that can yield good basic information.

In general the methodology applied has proved to be very useful, allowing to obtain a deep comprehension of a complex process in a relatively rapid and cost-less way. The key point of this methodology is represented by the chemometric approach, that provides a landmark over which it is possible setting and hence optimizing the experimental conditions for the analytical techniques employed. These last can include not only UV-visible spectroscopy and Mass spectrometry, as well as in this work, but several other techniques (such as HPLC-DAD, GC-MS, etc....) depending on the nature of samples.

Through this study a new methodology has been acquired with the possibility of future applications in the cultural heritage analysis.

CONSIDERAZIONI CONCLUSIVE

Lo scopo dello studio presentato era quello di *sviluppare una metodologia analitica capace di determinare differenti composti presenti in un campione senza segnali analitici specifici*. Questa metodologia è stata utilizzata per l'analisi del processo di fotodegradazione dell'azo colorante Acid Red 97 in presenza di perossido d'ossigeno, H_2O_2, come ossidante.

L'analisi è stata condotta monitorando il processo di fotodegradazione mediante spettroscopia UV-visibile e impiegando metodi chemiometrici per il trattamento delle informazioni chimiche contenute negli spettri UV-vis raccolti durante il processo.

In particolare l'analisi è stata strutturata in tre punti principali connessi tra di loro:

1. trattamento chemiometrico dei dati relativi agli spettri UV-vis raccolti durante la degradazione mediante strumenti di analisi multivariata, come la Decomposizione a Valori Singoli (SVD), l'Analisi dei Fattori in Evoluzione (EFA) e la Risoluzione di Curva Multivariante (MCR-ALS);

2. analisi con spettrometria di massa (MS) di alcuni campioni rappresentativi, raccolti durante il processo di degradazione, al fine di identificare gli intermedi di degradazione e di proporre un cammino di reazione;

3. investigazione del ruolo della concentrazione dell'H_2O_2 nell'andamento della degradazione, essendo uno dei fattori che influenzano maggiormente il processo di fotolisi H_2O_2/UV.

L'analisi chemiometrica dei dati raccolti durante gli esperimenti ha fornito due risultati fondamentali:

- durante il processo di degradazione vengono prodotti vari composti che mostrano differenti comportamenti: si formano e consumano in tempi diversi, come si può estrapolare dall'EFA plot; presentano differenti concentrazioni come indicato dai relativi profili; infine, presentano assorbanze in differenti ranges di lunghezze d'onda come è visibile nei relativi profili spettrali. In questo

modo è stato possibile ottenere un primo inquadramento della natura chimica dei composti formatisi;

- ha permesso di determinare che l'esperimento più lento è quello condotto senza H_2O_2, vale a dire Exp1, che consente pertanto di visualizzare meglio l'evoluzione del processo e, in particolare, i tempi in cui ogni intermedio si forma.

Questi risultati sono stati utilizzati per mettere a punto l'analisi in spettrometria di massa e per investigare l'influenza della concentrazione dell'H_2O_2.

L'EFA plot si è rivelato uno strumento fondamentale per la selezione di sei tempi del processo in corrispondenza dei quali raccogliere sei campioni che fossero i più rappresentativi delle differenti situazioni chimiche presenti nel corso del processo di degradazione dell'Exp1.

L'analisi spettrometrica di massa fu eseguita sui sei campioni suddetti e ha permesso di postulare un cammino di reazione per la degradazione svoltasi nell'Exp1, che potrebbe essere descritto come segue:

- il processo inizia dal colorante A.R.97 non trattato;
- inizialmente il colorante viene ossidato con la conseguente formazione di composti ad alto peso molecolare;
- il secondo step è caratterizzato dalla rottura dei legami azo e si ha la formazione di composti a peso molecolare intermedio;
- alla fine si formano prodotti di degradazione corrispondenti a composti aromatici a basso peso molecolare.

Segue che durante il processo due differenti intermedi di degradazione vengono prodotti. Questi sono poi consumati conseguentemente alla formazione dei prodotti di degradazione.

Dall'analisi dell'*Efficienza di decolorizzazione (%)* risulta che il processo di degradazione più rapido avviene durante l'Exp2, vale a dire con una concentrazione intermedia di H_2O_2 pari a 0.02 M. Senza ossidante la degradazione si presenta molto più lenta come nel caso dell'Exp1, mentre usando alte concentrazioni di H_2O_2 il processo viene inibito con un conseguente rallentamento della degradazione del colorante, come avviene nell'Exp3, dove è stato impiegato H_2O_2 0.05 M. L'inibizione del processo può essere attribuita all'eccesso di H_2O_2 che, reagendo con i radicali ossidrilici OH•, porta

alla produzione di radicali idroperossili $HO_2\bullet$, che non contribuiscono alla degradazione ossidativa.

L'impiego della spettroscopia UV-visibile è sembrato essere il fattore limitante della metodologia sviluppata a causa della bassa selettività della tecnica. Questo si è mostrato evidente soprattutto per quanto concerne l'Exp4, in cui è stato usato H_2O_2 0.1 M, e durante la determinazione degli intermedi di degradazione. In quest'ultimo caso non è stato possibile distinguere i due intermedi chimici a causa della simile struttura molecolare e, pertanto, della simile assorbanza. Nell'Exp4 l'elevata velocità della degradazione che caratterizza i primi minuti del processo ha fatto si che le informazioni relative ai primi minuti non fossero sufficienti per poter sviluppare una buona analisi chemiometrica. Occorre comunque ricordare che la spettroscopia UV-visibile rappresenta una tecnica analitica semplice, veloce e a basso costo, capace di fornire un primo inquadramento basilare del sistema oggetto di studio.

In generale la metodologia applicata ha dimostrato d'essere particolarmente funzionale, permettendo di comprendere un processo complesso in un modo relativamente rapido ed economico. Il cuore di questa metodologia è rappresentato dall'approccio chemiometrico, che fornisce un punto di riferimento a partire dal quale è possibile impostare e quindi ottimizzare le condizioni sperimentali per le tecniche analitiche utilizzate. Entro quest'ultime si possono annoverare non solo la spettroscopia UV-visibile e la Spettrometria di Massa, ma bensì differenti altre tecniche (ad esempio: HPLC-DAD, GC-MS, ecc…) in funzione della natura dei campioni e del sistema da analizzare.

Grazie a questo studio si è potuto acquisire una metodica di cui non si escludono possibili future applicazioni nell'ambito dell'analisi dei beni storico-artistici.

- 6 -

ANNEX

6.1   BASIC PRINCIPLES OF CHEMOMETRICS

6.1.1   Structure of data

The employment of chemometric allows "to extract the maximum relevant chemical information by analysing chemical data" [45]. In general in order to extract this information, chemometric tools are applied on experimental data structured in tables, called matrices.

A matrix $\mathbf{X}$ is constituted by n rows and m columns (fig.6.1b) and in general is written as $\mathbf{X}(n \times m)$. Conventionally rows are assigned to *objects* or samples and columns to *variables* or measurements which describe severally and individually each object. For a given matrix its number of rows and its number of columns are its *dimensions*.
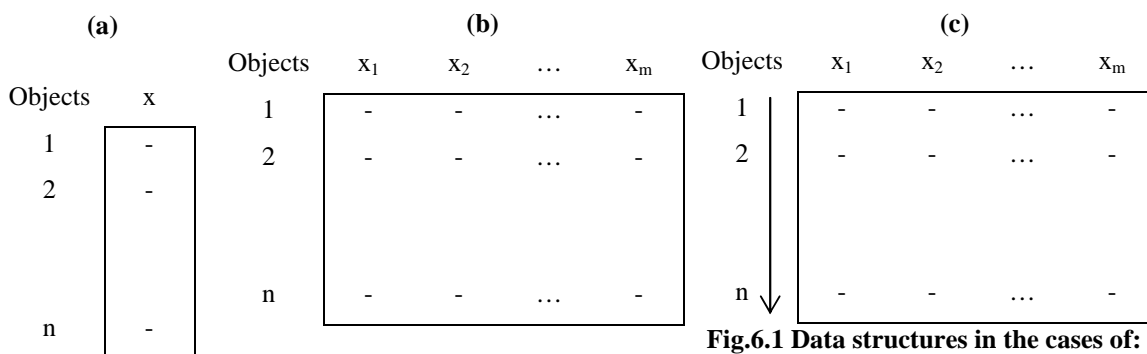
Fig.6.1 Data structures in the cases of:
univariate data (a), multivariate data (b)
and multivariate data subjected to an order (c).

Experimental data can be distinguished in: *univariate data*, if one variable *x* describes a set of objects (fig.6.1a) and in *multivariate data* when the same individual object is described by many variables (fig.6.1b). In some instances the objects are ordered in function of a variable increasing or decreasing, such as time or pH (fig.6.1c).

6.1.2 Vectors and matrices

A data matrix consists of sub-sets of data for the different variables (column-wise) and for the objects (row-wise). These subsets are called *vectors*. Fig.6.2 shows the elements constituting a matrix.

For convention a vector is a *column-vector*, while a row is considered a transpose of a column vector. The *rank* of a matrix is defined as the minimum number of row or column vectors linearly independent.

A vector is a linear arrangement of numbers and geometrically it can be represented as a directed line segment in a plane the axes of which are associated with the variables (fig.6.3).
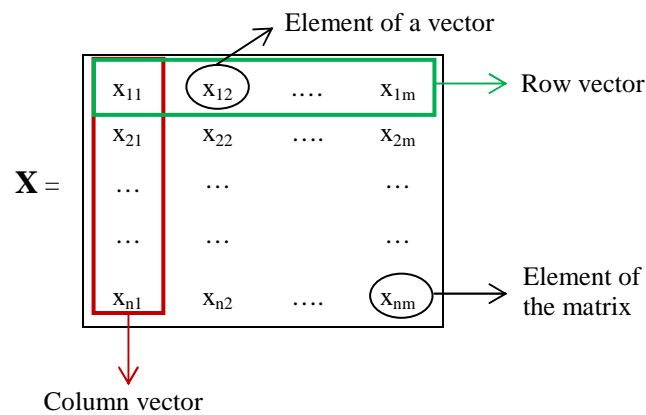
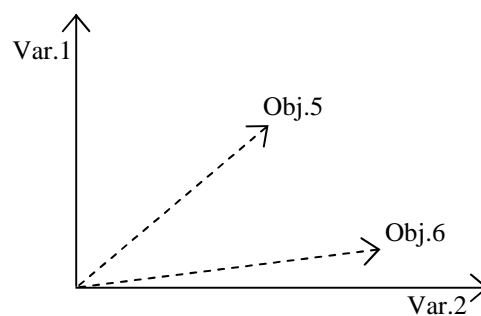**Fig.6.2 Principal elements constituted a matrix X (m x n).**

Fig.6.3 Representation of vectors in a variable space.

In this case since there is a column for each variable, it can infer that the objects of rows are represented in *column space* or *variable space*. In the same way it is possible to represent the variables in *row space* or *objects space*. It follows that a matrix, as it is a collections of vectors, allows to represent data sets in multivariate space.

6.1.3 Multivariate analysis of data

6.1.3.1 Principal components analysis (PCA)

When multivariate data must be handled to extrapolate from them much information as possible, it is necessary to plot the data using as many dimensions as there are variables. It is clear that for more than three dimensions a visual evaluation of the data becomes very difficult.

The Principal Component Analysis (PCA) is one of the most useful and used technic which allows to overcome this problem, reducing the dimensionality of multivariate data. Therefore it presents as an important tools for the multivariate analysis of data, which permits to explain the experimental variation observed.

PCA is a mathematic procedure that uses an orthogonal transformation to convert a set of observations of possible correlated variables into a set of values of linearly uncorrelated variables, called *principle component* or *factor* [45]. This transformation occurs in a way that the first principal component has the largest possible variance.

Figures 6.4a and 6.4b show the situation in which only two variables (Var.1 and Var.2) are present and the aim is reducing them to one. To do this the points are projected from the two-dimensional space to the one-dimensional space of the line. In fig.6.4a the projections on the line not yield much information about the structure of the original data set: it is no possible to observe the presence of two groups of data.

Instead in fig.6.4b the projections allow to determine the most important characteristic of data structure. It follows that a good direction to draw the line is along the axis of largest variation in the data and, therefore, that the first principal component,

PC1, accounts for most information. The unexplained variation is represented by the second principal component, PC2, which is orthogonal to the first.

In the case described, since there are only two variables, the two components described entirely the original data and each component is a linear combination of the original variables.
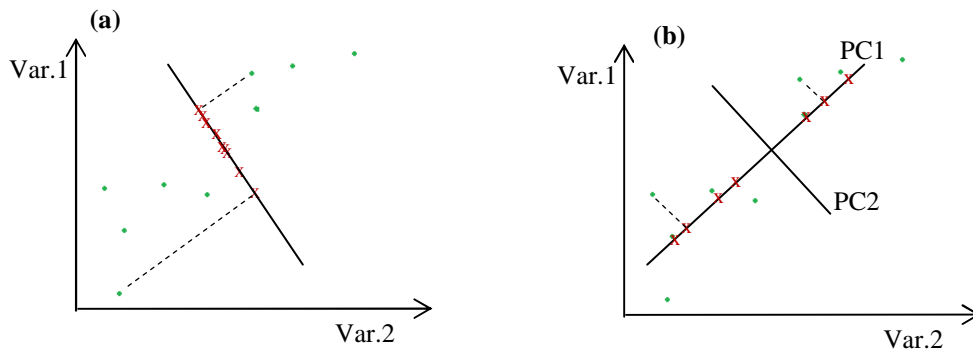

Fig.6.4 Projections from two to one dimension. In (a) the information is lost. In (b) the formation is represented by the two principal components PC1 and PC2.

6.1.3.2 Scores and loadings

The projections of the point from the original space defined by Var.1 and Var.2 on PC1 are called the *scores* (of the objects) on PC1. The same can be said for PC2.

These projections on the plane of PC1 and PC2 can be computed and shown in a plot called *score plot*, in which it is possible visualize the relationship among objects.

The scores on the principal components are a weighted sum of the original variables. In this sum the weight, that contain information about the variables, are called *loadings*, so that in general the followed equation is given:

$$s_{ip} = \sum_{j} v_{ip} \cdot x_{ij}$$

(Eq.6.1)

where s_{ip} is the score of the *i*th object along a principal component PCp, v_{ip} is the loading of variable *j* on PCp and x_{ij} is the value of the *i*th object for the original variable *j*.

In matrix notation:

$$\mathbf{T} = \mathbf{X}\,\mathbf{V} \qquad\qquad\qquad (Eq.6.2)$$

where $\mathbf{T}$(n x m) is the matrix of scores, $\mathbf{X}$(n x m) is the matrix of original variables and $\mathbf{V}$(m x m) is the matrix of loadings. In this way the principal components are related with the original variables.

As done for the scores, also the loadings can be displayed in two-dimensional *loading plot*. In this case the relationship between variables is emphasised.

6.1.3.3 Singular Value Decomposition (SVD): eigenvectors and eigenvalues

Mathematically PCA determines principal components through the *diagonalization* of the covariance matrix $\mathbf{S}$ of $\mathbf{X}$, i.e. the original data matrix.

The term diagonalization means that the *eigenvectors* and the *eigenvalues* of $\mathbf{S}$ are calculated employing the algorithm od *Singular Value Decomposition* (SVD).

According to SVD any matrix $\mathbf{X}$ can be decomposed as:

$$\mathbf{X} = \mathbf{U}\,\mathbf{W}\,\mathbf{V}^{\mathbf{T}} \qquad\qquad\qquad (Eq.6.3)$$

where $\mathbf{U}$(n x m) is related to the scores of the object, $\mathbf{V}$(m x m) to the loading of the original variables and $\mathbf{W}$(m x m) is a diagonal matrix related to the variation explained by successive components.

Matrix $\mathbf{W}$ can be described as a weight matrix in which the weights are ranked in descending order along the diagonal. This matrix is called the *singular values matrix* and its diagonal elements are the singular value w_m.

In PCA, when the SVD algorithm is applied on covariance matrix instead of $\mathbf{W}$ is used $\mathbf{\Lambda}$. This last is a diagonal matrix called the *eigenvalues matrix*, of which diagonal elements are the eigenvalues λ_m. Between singular values and eigenvalues there is the relation:

$$\lambda_{m\,=}\,w_m{}^2 \qquad\qquad\qquad (Eq.6.4)$$

that in matrix notation is expressed as $\mathbf{\Lambda} = \mathbf{W}^2$.

Each eigenvalue is associated with a principal component, so that the eigenvalues represent the variation of the data along the single component. It is clear that eigenvalues explain successively less information, since they are associated with successively less important principal components. In particular the sum of eigenvalues is equal to the sum of all the variance along the principal components, the important of which can be obtained by the following:

$$\text{Expl.Var. \%} = \frac{\lambda_j}{\sum\limits_{j} \lambda_{jm}} \cdot 100 \qquad \text{(Eq.6.5)}$$

$\mathbf{V}$ and $\mathbf{U}$ are orthonormal matrices. The columns of matrix $\mathbf{V}$ are the successive eigenvectors for the components and the rows are the loadings of the original variables. $\mathbf{U}$ is the normed score matrix, so that multiplying the normed score matrix $\mathbf{U}$ with the weight matrix $\mathbf{W}$ the score matrix $\mathbf{T}$ is obtained:

$$\mathbf{T} = \mathbf{U}\,\mathbf{W} \qquad \text{(Eq.6.6)}$$

so that, for the case where PCA is done on S, the following is turned out:

$$\mathbf{T} = \mathbf{S}\,\mathbf{V} \qquad \text{(Eq.6.7)}$$

Therefore any matrix can be decomposed into a set of matrices: two orthonormal matrices, $\mathbf{U}$ and $\mathbf{V}$, and one diagonal matrix $\mathbf{W}$. $\mathbf{U}$ describes the locations of the objects in space, $\mathbf{V}$ describes the relation between the old and new variables and $\mathbf{W}$ describes the amount of variance present in each singular values (or eigenvalues, since they are related) [45].

6.2   USE OF SVD DURING THE STUDY

For the purpose followed in this thesis, more attention has been put in matrix **W** that has provided the singular values for the four matrices handled during the study. These singular values are exploited for:

- determine the number of significant components with a simple comparison between the singular values of dye degradation matrix and that one of the blank degradation matrix;

- determine the number of significant components calculating the explained variance for each singular value with Eq.6.5 and plotting it in a scree plot;

- determine the background level in the EFA plot obtaining the relative eigenvalues and employing the Eq. 6.4.

- 7 -

REFERENCES

1. Khehra, M.S., et al., *Biodegradation of azo dye C.I. Acid Red 88 by an anoxic-aerobic sequential bioreactor*, Dyes and Pigments, 2006, 70(1), pp. 1-7.

2. Tsantaki, E., et al., *Anodic oxidation of textile dyehouse effluents on boron-doped diamond electrode*, Journal of Hazardous Materials, 2012, 207-208, pp. 91-96.

3. Fernández, C., M.P. Callao, and M.S. Larrechi, *Kinetic analysis of C.I. Acid Yellow 9 photooxidative decolorization by UV-visible and chemometrics*, Journal of Hazardous Materials, 2011, 190(13), pp. 986-992.

4. Patnaik, P., *A comprehensive guide to the hazardous properties of chemical substances*, 3th Edition ed. 2007, New Jersey, Wiley.

5. *Lecture notes from the course "Chimica dei pigmenti e dei coloranti organici" (prof. O. De Lucchi, Ca' Foscari University),* a.y. 2010-2011.

6. www.spectroscopynow.   [cited 24/02/2012].

7. www.color-index.com. *Color Index web-site*.   [cited 26/02/2012].

8. www.aatcc.org. *American Association of Textile Chemists and Colorists*.   [cited 26/02/2012

9. www.sdc.org.uk. *Society   of   Dyer   and   Colorists*.   [cited   26/02/2012].

10.   IARC, ed. *Some aromatic amines, organic dyes, and related exposures*, IARC Monographs on the Evaluation of Carcinogenic Risks to Human, 2010, 99, Lyon (France).

11.   A. Maximova, B.K., *Equilibrium and kinetics of adsorption of basic dyes onto perfil from aqueous solutions*, Journal of the University of Chemical Technology and Metallurgy, 2008, 43(1), pp. 101-108.

12.   Wojnárovits, L. and E. Takács, *Irradiation treatment of azo dye containing wastewater: An overview*, Radiation Physics and Chemistry, 2008, 77(3), pp. 225-244.

13.   Forgacs, E., T. Cserháti, and G. Oros, *Removal of synthetic dyes from wastewaters: a review,* Environment International, 2004, 30(7), pp. 953-971.

14.   Oh, S.W., et al., *Detection of carcinogenic amines from dyestuffs or dyed substrates.* Dyes and Pigments, 1997, 33(2), pp. 119-135.

15.   N. Puvaneswari, J.M., P. Gunasekaran, *Toxicity assessment and microbial degradation of azo dyes,* Indian Journal of Experimental Biology, August 2006, 44, pp. 618-626.

16.   Manjinder Singh Khehra, H.S.S., Bhupinder Singh Chadha, Swapandeep Singh Chimni, *Biotreatment of synthetic textile wastewater using anoxic-aerobic sequential bioreactor* 5th International exhibition and conference on environmental technology, 2005, Exhibition Centre Helexpo, Athens, Greece.

17.   Fernández, C., M.S. Larrechi, and M.P. Callao, *An analytical overview of processes for removing organic dyes from wastewater effluents*, TrAC Trends in Analytical Chemistry, 2010, 29(10), pp. 1202-1211.

18.   Harrelkas, F., et al., *Treatment of textile dye effluents using coagulation-flocculation coupled with membrane processes or adsorption on powdered activated carbon,* Desalination, 2009, 235(1-3), pp. 330-339.

19.   Gómez, V., M.S. Larrechi, and M.P. Callao, *Kinetic and adsorption study of acid dye removal using activated carbon,* Chemosphere, 2007, 69(7), pp. 1151-1158.

20.   Gómez, V. and M.P. Callao, *Modeling the adsorption of dyes onto activated carbon by using experimental designs,* Talanta, 2008, 77(1), pp. 84-89.

21. Ong, S., et al., *Combination of adsorption and biodegradation processes for textile effluent treatment using a granular activated carbon-biofilm configured packed column system,* Journal of Environmental Sciences, 2008, 20(8), pp. 952-956.

22. Hai, F.I., et al., *Application of a GAC-coated hollow fiber module to couple enzymatic degradation of dye on membrane to whole cell biodegradation within a membrane bioreactor*, Journal of Membrane Science, 2011, 389, pp. 67-75.

23. Zahrim, A.Y., C. Tizaoui, and N. Hilal, *Coagulation with polymers for nanofiltration pre-treatment of highly concentrated dyes: A review,* Desalination, 2011, 266(1-3), pp. 1-16.

24. Saratale, R.G., et al., *Bacterial decolorization and degradation of azo dyes: A review*, Journal of the Taiwan Institute of Chemical Engineers, 2011, 42(1), pp. 138-157.

25. Pearce, C.I., J.R. Lloyd, and J.T. Guthrie, *The removal of color from textile wastewater using whole bacterial cells: a review*, Dyes and Pigments, 2003, 58(3), pp. 179-196.

26. Elmorsi, T.M., et al., *Decolorization of Mordant red 73 azo dye in water using H2O2/UV and photo-Fenton treatment*, Journal of Hazardous Materials, 2010, 174(1-3), pp. 352-358.

27. Behnajady, M.A., N. Modirshahla, and H. Fathi, *Kinetics of decolorization of an azo dye in UV alone and UV/H2O2 processes*, Journal of Hazardous Materials, 2006, 136(3), pp. 816-821.

28. Gül Ş., and Ö. Özcan-Yıldırım, *Degradation of Reactive Red 194 and Reactive Yellow 145 azo dyes by O_3 and H_2O_2/UV-C processes*, Chemical Engineering Journal, 2009, 155(3), pp. 684-690.

29. O. Legrini, E.O., A. M. Braun, *Photochemical processes for water treatment*, Chemical Reviews, 1993, 93(2), pp. 671.

30. Galindo, C., P. Jacques, and A. Kalt, *Photodegradation of the aminoazobenzene acid orange 52 by three advanced oxidation processes: UV/H_2O_2, UV/TiO_2 and VIS/TiO_2: Comparative mechanistic and kinetic investigations*, Journal of Photochemistry and Photobiology A: Chemistry, 2000, 130(1), pp. 35-47.

31. Fernández, C., M.S. Larrechi, and M.P. Callao, *Modeling of the simultaneous photodegradation of Acid Red 97, Acid Orange 61 and Acid Brown 425 using factor*

screening and response surface strategies, Journal of Hazardous Materials, 2010, 180(1-3), pp. 474-480.

32.   Fernández, C., M.S. Larrechi, and M.P. Callao, *Study of the influential factors in the simultaneous photocatalytic degradation process of three textile dyes*, Talanta, 2009, 79(5), pp. 1292-1297.

33.   Barbusiński, K., *Fenton reaction Controversy concerning the chemistry*, Ecological Chemistry and Engineering, 2009, 16(3), pp. 347-358.

34.   Kansal, S.K., M. Singh, and D. Sud, *Studies on photodegradation of two commercial dyes in aqueous phase using different photocatalysts*, Journal of Hazardous Materials, 2007, 141(3), pp. 581-590.

35.   R. Kellner, J.M.M., M. Otto, M. Valcarcel, H. M. Widner, *Analytical Chemistry*, ed. A.m.a.t.a. Science, 2004, Wiley-VCH.

36.   Higson, S.P.J., *Analytical chemistry*, 2004, New York, Oxford.

37.   Es'haghi, Z., *Photodiode array detection in clinical applications; quantitative analyte assay advantages, limitations and disadvantages*, in *Photodiodes - Communications, Bio-Sensings, Measurements and High-Energy Physics*, InTech Editor, September 2011.

38.   Fernández, C., et al., *Multisyringe chromatography (MSC) using a monolithic column for the determination of sulphonated azo dyes*, Talanta, 2010, 82(1), pp. 137-142.

39.   Şahin S., C. Demir, and Ş. Güçer, *Simultaneous UV-vis spectrophotometric determination of disperse dyes in textile wastewater by partial least squares and principal component regression*, Dyes and Pigments, 2007, 73(3), pp. 368-376.

40.   Gross, J.H., ed. *Mass spectrometry: a textbook*, 2004, Springer, Berlin.

41.   Somogyi, A., *Mass spectrometry instrumentation and techniques*, in *Medical applications of mass spectrometry*, 2007, Elsevier, Amsterdam.

42.   Christopher G. Herbert, R.A.W.J., *Mass Spectrometry Basics*, 2003, New York, CRC Press.

43.   Schröder, H.F., *Polar organic pollutants from textile industries in the wastewater treatment process â€" biochemical and physicochemical elimination and degradation monitoring by LC-MS, FIA-MS and MS-MS*, TrAC Trends in Analytical Chemistry, 1996, 15(8), pp. 349-362.

44.   Holčapek, M., K. Volná, and D. Vaněrková, *Effects of functional groups on the fragmentation of dyes in electrospray and atmospheric pressure chemical ionization mass spectra.* Dyes and Pigments, 2007, 75(1), pp. 156-165.

45.   D.L. Massart, B.G.M.V., L.M.C. Buydens, S. De Jong, P.J. Lewi, J. Smeyers-Verbeke, *Handbook of Chemometrics and Qualimetrics: Part A*, Data handling in science and technology - volume 20A, 1997, Amsterdam, Elsevier.

46.   Roma, T., *Multivariate curve resolution applied to second order data*, Chemometrics and Intelligent Laboratory Systems, 1995, 30(1), pp. 133-146.

47.   de Juan, A. and R. Tauler, *Chemometrics applied to unravel multicomponent processes and mixtures: Revisiting latest trends in multivariate resolution*, Analytica Chimica Acta, 2003, 500(1-2), pp. 195-210.

48.   R. Tauler, A.D.J., R. Gargallo, *Analisis y resolucion de factores en quimica*, in *Temas avanzados de quimiometria*, 2007, Universitat de les Illes Balears, Palma.

49.   D.L. Massart, B.G.M.V., L.M.C. Buydens, S. De Jong, P.J. Lewi, J. Smeyers-Verbeke, *Handbook of Chemometrics and Qaulimetrica: Part B*, Data handling in science and technology - volume 20B, 1997, Amsterdam, Elsevier.

50.   Keller, H.R. and D.L. Massart, *Evolving factor analysis*, Chemometrics and Intelligent Laboratory Systems, 1992, 12(3), pp. 209-224.

51.   Maeder, M., et al., *2.16 - Two-Way Data Analysis: Evolving Factor Analysis*, in *Comprehensive Chemometrics*, 2009, Elsevier, Oxford. pp. 261-274.

52.   Jaumot, J., et al., *A graphical user-friendly interface for MCR-ALS: a new tool for multivariate curve resolution in MATLAB*, Chemometrics and Intelligent Laboratory Systems, 2005, 76(1), pp. 101-110.

53.   Amigo, J.M., et al., *A mixed hard- and soft-modeling approach to study and monitor enzymatic systems in biological fluids*, Analitica Chimica Acta, 2006, 567(2), pp. 245-254.

54. D'Ischia, M., *La chimica organica in laboratorio*, 2002, Padova, Piccin Nuova Libraria S.p.A.

55. Amrhein, M., et al., *Calibration of spectral reaction data*, Chemometrics and Intelligent Laboratory Systems, 1999, 46(2), pp. 249-264.

ACKNOWLEDGEMENT

grande avventura durata anni! Grazie per le ore passare assieme, il sostegno, il coraggio che mi avete dato, per le risate e gli sprizetti bevuti assieme.

E arriviamo al ponte della Libertà, il ponte che ti conduce fuori, nel mondo.
Questa tesi infatti è nata durante gli otto mesi trascorsi a Tarragona (Catalunya), è il frutto del mio Erasmus e potete immaginare quanti ricordi, immagini e riflessioni sono raccolti tra queste pagine oltre al lavoro e ai risultati scientifici. Mille volti di molte persone che in misura diversa mi hanno aiutato a portare a termine questo sudato lavoro.

El primero " muchas gracias!" es para las Professoressas M. Callao y S. Larrecchi, que me han seguido en estos ocho meses de trabajo, compriendendo tambien las mis primeras dificultas con la nueva realidad en la que empezè a vivir.
A seguir ella, la primera sonrisa y el mi primer apoyo en el Dipartimento, Cristina! Una persona locamente increible, de verdad un placer conocerla. Como fue un placer trabajar en el Dipartimento de Quimometria, Qualimetria y Nanosensores de la URV, la mi segunda casa, donde ya desde los primeros dias fui recibida como una de la "familia", la mi familia catalana:
Thomas, el mi hermanito y primer amigo, que me abri las puertas de Reus!
Alex, amigo amable y siempre disponible!
Maribel, la mi compañera de despacho y mamma personal!
Idoia, el mi primer: "Anem a fer un cafe?" (Si, con mucho gusto!), que me ha hecho encontrar los lugares mas bonitos de Tarragona y la musica catalana mas amable!
Marta C. y Marta P. siempre con las sonrisas!
Xavi, Santi, Pancho, Pascal, Maria!, Jad, y los de mas!

MUCHAS GRACIAS A TODOS VOSOTROS! Y FINS DESPRES AMICS!

Y los amigos fuera da la URV?! Es poco decir que en ellos encontrè el mundo!
Cada persona me donó algo, algo para emparar un poco mas de la vida, de mi. Las primeras caras de la mi rara esistencia en Tarragona, eran mucho diferentes: una cara de un joven poeta rumano, aquella de un loco fotografo polaco y la otra de un chino particular, amante de la cultura hispanica. Dani, Kuba, Hao...gracias, porque en vostros encontrè los primeros y verdaderos vinculos en una tierra enstranjera.
Un gracias especial a los mi compañeros de piso, Carlos y Deborah. Mis hermanos y apoyos sobretodo en los ultimos meses, en cuyos he tenido que poner mas esfuerzo en el mi trabajo.
Pero siempre estavan ellos, mis amigos....de verdad he tenido mucha suerte en el encontrar personas asi especial que me comprendeban cuando estaba de todo agotada para la thesis, cuando pensabo de no poder aguantar mas y de no acabar nunca:
Anna y Laura, locas chicas alemanas
Alex, italiano todo particular (no te preocupes, te dono la traducion en ingles de todo esto)
Mary, un entero barrio de Manchester en Tarragona! (madly sweet)
Andrea y Marco, compañeros de piso para tres dias

Luca y Marion, amigo del almuerzo y amiga de aventura
Maria, darling friend of chatting
Ali, the best neighbour

Paride e Lorenzo! Scusate ma qua la lingua del cuore è d'obbligo. I miei Amici, i ponti dell'Accademia della mia vita a Tarragona, legami nati provvisori che rimarranno per sempre. Tosati, oltre ad aiutarmi, sostenermi, farmi ridere (tanto), cantare, ballare, coinvolgermi in avventure folli (Provenza'! ci sei anche tu qua eh!) mi avete ricordato quanto bella è la mia terra e quanto è importante trovare degli amici, veri. Non so se ce l'avrei fatta senza di voi, le mie valvole di sfogo. Se veden a Venexia para bever uno sprizett!

GRACIAS, THANK YOU, MULŢUMIRI, DZIĘKUJĘ, DANKESCHÖN, MERCI!

GRAZIE!!!!

Università Ca' Foscari - Venezia

ESTRATTO PER RIASSUNTO DELLA TESI DI LAUREA E DICHIARAZIONE DI CONSULTABILITA'(*)

Il sottoscritto/a **DANIELA ISEPPI**

Matricola n. **811106** Facoltà **SCIENZE MATEMATICHE FISICHE E NATURALI**

iscritto al corso di ○ laurea ◉ laurea magistrale/specialistica in:

Scienze Chimiche per la Conservazione e il Restauro

Titolo della tesi (**): **Chemometric analysis of the photooxidative decolorization of the azo dye Acid Red 97**

DICHIARA CHE LA SUA TESI E':

◉ Consultabile da subito ○ Consultabile dopo ___ mesi ○ Non consultabile

○ Riproducibile totalmente ◉ Non riproducibile ○ Riproducibile parzialmente

Venezia, **04/06/2012** Firma dello studente _____

(spazio per la battitura dell'estratto)

In questo studio si è voluto sviluppare una metodologia capace di analizzare processi complessi senza iniziali segnali analitici specifici, utilizzando in sinergia metodi chemiometrici e diverse tecniche analitiche. In particolare nel presente lavoro di tesi è stato analizzato il processo di fotodegradazione dell'azocolorante Acid Red 97. La degradazione è stata condotta mediante un metodo di ossidazione avanzata (AOP) che prevede l'uso di radiazione ultravioletta in presenza di H_2O_2 come agente ossidante. Il processo di degradazione è stato prima monitorato mediante spettroscopia UV-visibile. I dati raccolti sono stati poi trattati per mezzo del metodo multivariante MCR-ALS (Multivariate Curve Resolution with Alternative Least Square). In tale approccio chemiometrico il numero delle fonti di variabilità chimica sono individuate applicando l'algoritmo di Decomposizione a Valore Singolo (SVD) e l'analisi dei Fattori in Evoluzione (EFA). Le informazioni ottenute sono state poi completate dall'analisi in Spettrometria di Massa (MS) di alcuni campioni raccolti durante il processo di degradazione, al fine di identificare i possibili intermedi di degradazione e di proporre un cammino di reazione. Infine, è stato investigata l'influenza della concentrazione di H_2O_2 nel processo di degradazione mediante il calcolo dell' Efficienza di Degrazione (%).

(*) Da inserire come ultima pagina della tesi. L'estratto non deve superare le mille battute
(**) il titolo deve essere quello definitivo uguale a quello che risulta stampato sulla copertina dell'elaborato consegnato al Presidente della Commissione di Laurea

Università Ca' Foscari - Venezia

Informativa sul trattamento dei dati personali

Ai sensi dell'art. 13 del D.Lgs. n. 196/03 si informa che il titolare del trattamento dei dati forniti è l'Università Ca' Foscari - Venezia.

I dati sono acquisiti e trattati esclusivamente per l'espletamento delle finalità istituzionali d'Ateneo; l'eventuale rifiuto di fornire i propri dati personali potrebbe comportare il mancato espletamento degli adempimenti necessari e delle procedure amministrative di gestione delle carriere studenti.

Sono comunque riconosciuti i diritti di cui all'art. 7 D. Lgs. n. 196/03.